

Nesting and Developmental Biology of the Cleptoparasitic Bee *Stelis ater* (Anthidiini) and Its Host, *Osmia chalybea* (Osmiini) (Hymenoptera: Megachilidae)

Authors: Rozen, Jerome G., and Hall, H. Glenn

Source: American Museum Novitates, 2011(3707) : 1-38

Published By: American Museum of Natural History

URL: <https://doi.org/10.1206/3707.2>

BioOne Complete (complete.BioOne.org) is a full-text database of 200 subscribed and open-access titles in the biological, ecological, and environmental sciences published by nonprofit societies, associations, museums, institutions, and presses.

Your use of this PDF, the BioOne Complete website, and all posted and associated content indicates your acceptance of BioOne's Terms of Use, available at www.bioone.org/terms-of-use.

Usage of BioOne Complete content is strictly limited to personal, educational, and non - commercial use. Commercial inquiries or rights and permissions requests should be directed to the individual publisher as copyright holder.

BioOne sees sustainable scholarly publishing as an inherently collaborative enterprise connecting authors, nonprofit publishers, academic institutions, research libraries, and research funders in the common goal of maximizing access to critical research.

Nesting and Developmental Biology of the Cleptoparasitic Bee *Stelis ater* (Anthidiini) and Its Host, *Osmia chalybea* (Osmiini) (Hymenoptera: Megachilidae)

JEROME G. ROZEN, JR.,¹ AND H. GLENN HALL²

ABSTRACT

Herein we provide the first account of the nesting biology of *Osmia* (*Helicosmia*) *chalybea* Smith and of its cleptoparasite *Stelis* (*Stelis*) *ater* Mitchell, a newly confirmed host association. The nesting behavior of *O. chalybea* is similar to what is known about other members of the subgenus *Helicosmia*, but novel information concerning egg eclosion and cocoon structure and function are reported. Eggs of *S. ater* were discovered both on the front surface of the host provisions as well as deeply buried in the pollen-nectar mixture. From numerous observations, larval *S. ater* attacks host immatures or conspecifics whenever encountered. Because young larvae are unable to crawl (perhaps a family characteristic), the hospicial individual may be in its third to fifth stadium or even in its second stadium, although none of the latter was certainly identified. Although usually a single cleptoparasitic egg or larva was found in a cell, two or three were occasionally observed there. The cocoon of *S. ater* was also examined closely. Although its construction differs in a number of ways from that of the host cocoon, the functions of both seem to be the same, i.e., excluding parasitic/parasitoid arthropods and preventing desiccation while allowing exchange of air with the outside through complex filtering devices at the front ends of cocoons. Known parasites/parasitoids in the area of study include the minute parasitoid wasp *Melittobia digitata* Dahms (Eulophidae) and the parasitic mite *Chaetodactylus rozeni* Klimov

¹ Division of Invertebrate Zoology, American Museum of Natural History (rozen@amnh.org).

² Department of Entomology and Nematology, University of Florida, Gainesville, FL (hgh@ufl.edu).

and O'Connor (the latter recovered from adults of *O. chalybea*). The nearly airtight cocoon fabric of both bee cocoons presumably assists immatures in maintaining their water balance through their many months of confinement.

Ovarian statistics for both species are presented and compared with congeners, and their eggs/mature oocytes are described. Both have five larval instars. Comparative taxonomic descriptions of last larval instars are presented, and mandibular shapes of other larval instars are diagrammed.

INTRODUCTION

Although melittologists have realized that cleptoparasitism in bees has evolved a number of times, consistent evidence is lacking as to how many times this has occurred among all families. In the Megachilidae, we conclude on the basis of adult anatomy that at least four distinct lineages arose independently (here identified by their most conspicuous genera): *Stelis* and relatives in Anthidiini (although *Hoplostelis* may well represent a separate cleptoparasitic origin); *Dioxys* and relatives in Dioxyini; *Coelioxys* and relatives in Megachilini; and *Bytinskia* (but perhaps others) in Osmiini (Michener, 2007). Biological information concerning taxa in each of these lineages is gradually accumulating that tests their monophyly. In general, similarities in modes of cleptoparasitism and anatomical modifications to hide eggs and kill host offspring argue for monophyletic origins, whereas disparity in these features favors an assumption of separate origins. The current study adds to our understanding of the genus *Stelis* by investigating for the first time details of the behavioral and anatomical cleptoparasitic adaptations of the larva of *S. (Stelis) ater* Mitchell, a species so rarely encountered that it was known heretofore from only three specimens, all females (fig. 14). We describe its egg, all larval instars, and cocoon. Former knowledge of the biology of the genus was recently summarized by Rozen and Kamel (2009), and we have found the paper by Torchio (1989b) on *S. (Stelis) montana* Cresson particularly informative in interpreting the biology of *S. ater* in the current study.

The host of *Stelis ater* in this study was *Osmia (Helicosmia) chalybea* Smith (fig. 11), the first confirmed host record for this cleptoparasite (Hall and Ascher, 2010). At the start of our study, we focused primarily on understanding the biology of the cleptoparasite, but we quickly recognized that little was known about the developmental and nesting biology of *O. chalybea*, despite a number of papers describing the nests of other species of the large, holarctic subgenus *Helicosmia* (Rust, 1974, and references therein; Hawkins, 1975; Michener, 2007). We therefore include an overview of its nest structure, details of its developmental biology, and descriptions of its cocoon and immature stages.

METHODS AND TERMINOLOGY

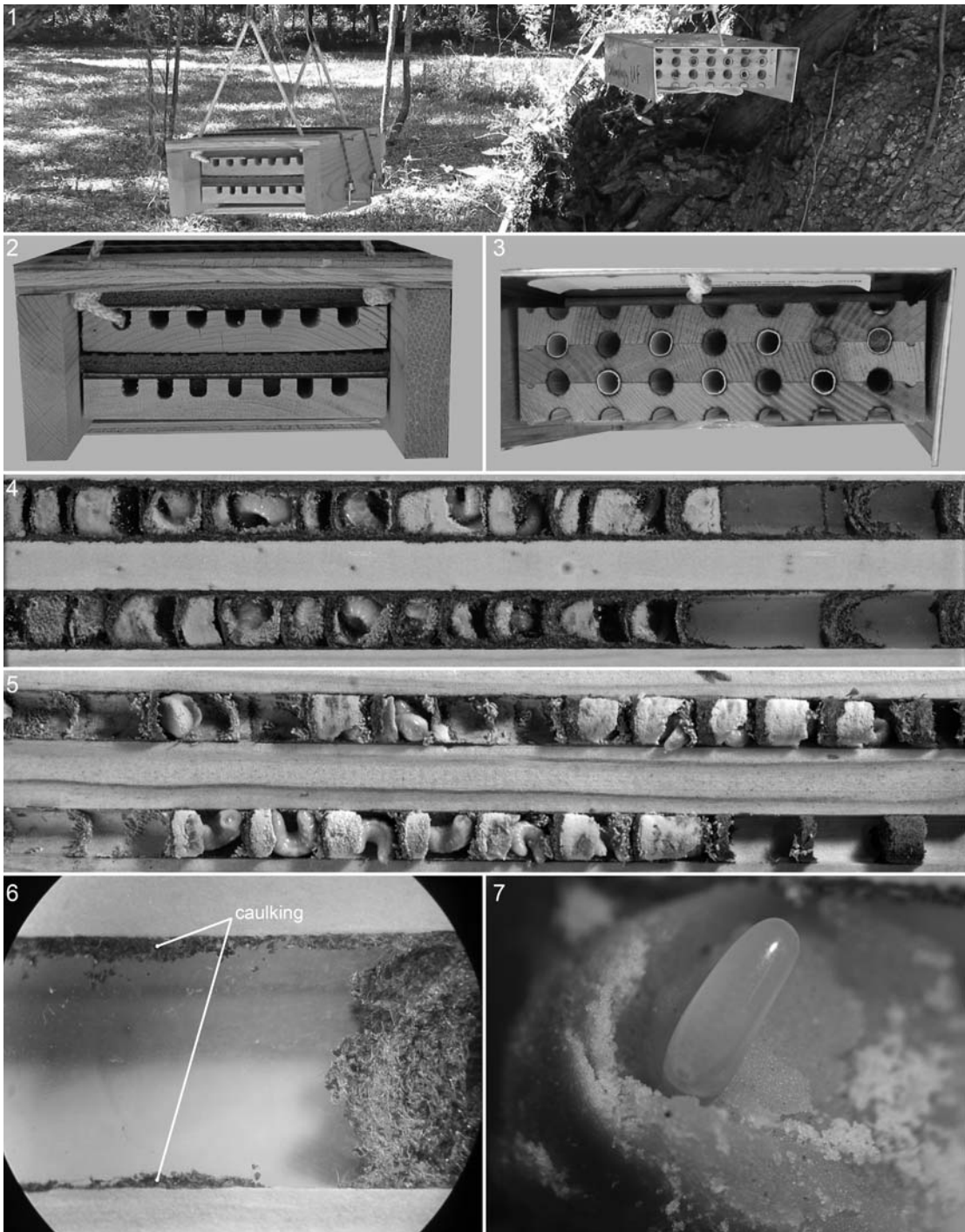
In 2006, H.G.H. was first to discover males of *Stelis ater* (Hall and Ascher, 2010), captured near Gainesville, Alachua Co., Florida. In early March 2009 he confirmed *S. ater* as a cleptoparasite of *Osmia chalybea* when both species emerged from trap nests. Cocoons still holding

S. ater adults adjacent to vacated *Osmia* cocoons were found inside the nests. The nests had been deployed in early spring of 2008, placed in screened emergence cages in early June after the nesting bees had closed the burrows, and kept at outside ambient temperatures until the following spring. At that time, recently vacated nests, intact *Stelis* cocoons, and new nests from 2009 were sent to J.G.R. In February and early March 2010, trap nests of two designs (below) were again deployed. The nests were monitored throughout the flight period of the bees, removed, opened, and examined. In early April, several nests were again sent to J.G.R. He visited Gainesville late that month.

The trap nests for this study were located at Kanapaha Prairie, a 300-hectare basin marsh surrounded by mesic hammock dominated by large live oaks (*Quercus virginiana* Mill.) (natural communities defined by the Florida Natural Areas Inventory: www.fnai.org/natcomguide_update.cfm), about 9.5 mi southwest of the Gainesville center. About 15 nest blocks were placed within a range of 100 m from a point on the west side of the prairie (29°33'09"N 82°26'09"W) and about 30 nest blocks were placed within 600 m from a point on the southeast side (29°32'14"N 82°25'02"W). The nests were attached to tree branches and trunks within the forested hammock bordering open areas, either the prairie itself, or smaller clearings, pasture or wetland basins within a few hundred meters of the prairie edge.

The two trap nest designs used for this study (fig 1.) differed in the shape and dimensions of their boreholes and produced different results. One design (hereafter referred to as "circular tunnels") offered *O. chalybea* cylindrical tunnels, 7 mm in diameter and 18 cm long (figs. 3, 6) cut in wooden blocks consisting of two rows each with seven cylindrical boreholes, designed to be split apart to reveal cell content (fig. 6) (commercially available 14-hole, 5/16" diameter, Binderboard® nests from www.pollinatorparadise.com). Some of the boreholes were lined with paper straws, and some were left unlined. The other design (hereafter referred to as U-shaped tunnels) consisted of blocks of wood in which a router was used to cut seven channels, each ≈9 mm (3/8" router bit) wide and deep, U-shaped in cross section (fig. 2), and 18 cm long. Because of a concern that these diameters were too large to attract *O. chalybea*, nests with ≈7.9 mm (5/16") channels were made available later in the spring. A pane of clear plastic was screwed in place over these channels to allow inspection of nest construction during the nesting season (fig. 4). Each trap nest had two blocks, each covered with a piece of dark foam, placed in a small open wooden shelter (fig. 2). All trap nests were deployed 1.0–2.5 m above ground surface at the sites by being suspended from branches so that nesting boreholes were approximately horizontal (fig. 1). As mentioned in the following section, the two types of trap nests produced notably different results irrespective of environment where deployed. We harvested and examined specimens from nests as required for the ongoing investigation.

Preserved larvae were examined first without treatment. The head was removed from the body, and both cleared in an aqueous solution of sodium hydroxide, stained with Clorazol Black E, and stored in glycerin on well slides. Because treatment in sodium hydroxide causes pigmentation loss, some specimens of *Stelis ater* were cleared with lactic acid at the suggestion of Lee H. Herman. Although such clearing takes longer, pigmentation is preserved thereby expediting interpretation of sclerite boundaries.



FIGURES 1–7. Trap nests used in the study of *Osmia chalybea* and *Stelis ater*. 1. Two trap nests deployed in the field. 2. Front end of U-shaped trap nest. 3. Front end of circular trap nest, showing circular openings to boreholes lined with paper straws and unlined; note that two exhibit nest closures. 4. U-shaped trap nest seen

Microphotographs of figures 12, 13, 15, 79, and 82–87 were taken with a Microptics-USA photographic system equipped with an Infinity Photo-Optic K-2 lens system. Other microphotographs were taken with a Cannon PowerShot SD880 IS handheld to the oculars of a Leitz stereomicroscope, vintage 1960, and a Zeiss compound microscope.

Eggs and larvae to be examined with a Hitachi S-4700 scanning electron microscope (SEM) were critical-point dried and then coated with gold/palladium. Cocoons did not require drying and were simply mounted on stubs and coated. X-ray and CT-scan radiographs were taken using a GE Phoenix c|tome|x.

Below, we first treat the nesting biology, including cocoon construction, of *Osmia chalybea*, because it is fundamental to understanding the biology of *Stelis ater*, which follows. Next, an account of ovarian statistics of both species is offered, and finally we present descriptions of immature stages of both species.

Pictures of cocoons are uniformly presented with front ends up, but in trap nests those of *Osmia chalybea* usually had their long axis horizontal while those of *Stelis ater* tended to have their long axis about 45° from horizontal with front ends elevated.

NESTING AND DEVELOPMENTAL BIOLOGY OF *OSMIA CHALYBEA*

NEST STRUCTURE: Nesting biology of *Osmia chalybea* is similar to the accounts of other *Helicosmia*. All species studied are cavity nesters (Michener, 2007; Müller, 2010; references in Hurd, 1979; Rust, 1974, and references therein). As reported for other species of *Helicosmia* (with an apparent exception of *O. (Helicosmia) caerulea* (Linnaeus) noted by Malyshev, 1935, and other species, unpublished information, personal commun., P. Torchio), cells of *O. chalybea* are arranged in a linear series, with cells separated by partitions of greenish masticated leaf tissue that when dried takes on a cardboard consistency. These partitions, or septa, are concave on the side facing the nest entrance and convex on the opposite side. Provisions of the cell in front of a partition are piled against it, and the *Osmia* female places her egg on the front surface of the provisions in the short open space between provisions and the next partition to be constructed, which will be either the rear of the next cell to be constructed or the start of a nest closure. A completed nest may have as many as 11 or 12 cells, dictated by the length of the borehole, although some completed nests have fewer cells. Nest closures normally consist of two septa similar to cell partitions with a small to large, open vestibular space between the two of them and between the inner one and the closure of the last cell constructed in the cell series. These nest closure septa are similar to partitions between cells but usually noticeably thicker though always concave on the side toward the nest entrance. Outer closures septa are

← from above demonstrating cells of irregular lengths and variable contents; nest opening to right. 5. Opened circular trap nest showing tunnels revealing regular placement of cell partitions (even though some cell contents had remained with top half of nest), nest entrance to right. 6. Close-up of vestibule of a tunnel in a U-shaped nest of *Osmia chalybea* showing masticated leaf material caulking cracks between clear plastic and wood. 7. Egg of same showing typical attachment of posterior end inserted into front surface of provisions.

often, but not invariably, flush with the front end of the tunnel (figs. 3, 4). Neither cell partitions nor nest closure septa exhibit a spiral pattern on the inner surface, as is often visible on mud closures of soil-nesting bee species.

Interestingly, in addition to providing masticated leaf material to construct partitions and later nest closures, females also use this material to caulk fine cracks formed where the clear plastic covers the wood of the block beneath on the U-shaped tunnels (as defined in the section on Methods and Terminology) (fig. 6) and on many cracks separating the upper and lower blocks of circle-shaped tunnels of trap nests. Intriguing is the realization that an adult bee could detect such a thin line and manipulate a fine line of material to it. It functions almost certainly to exclude mites and other parasites/parasitoids.

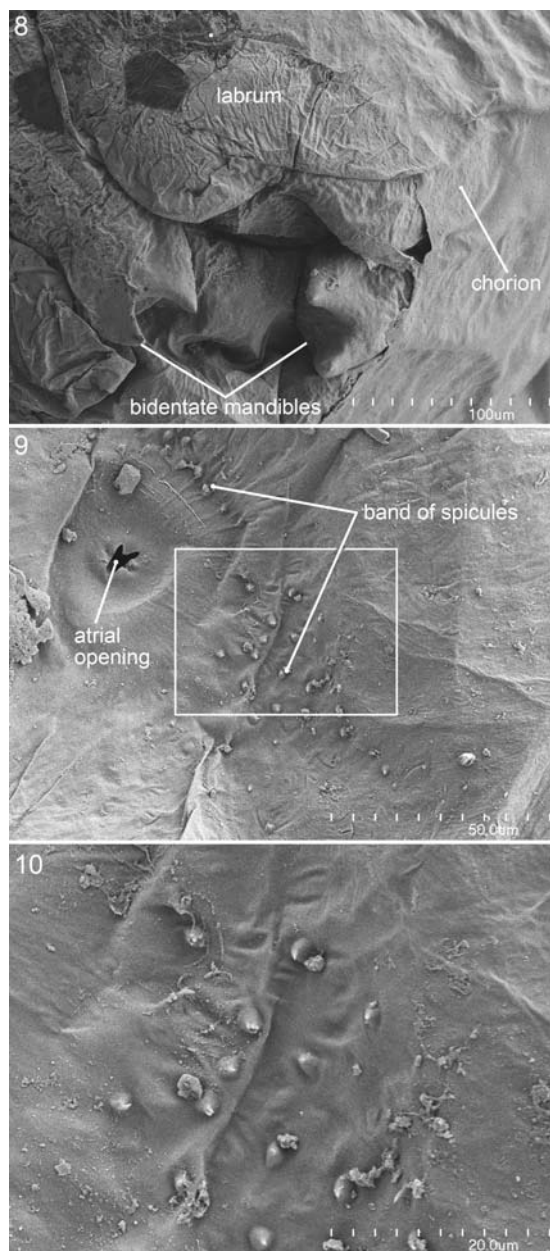
Cells in circular tunnels were 14–16 mm long, consistent in length, and usually each initially contained an egg and a uniform amount of provisions. However, cells in the 9.5 mm U-shaped tunnels were 3–15 mm long, thus varying extensively in length, with the shorter ones containing much less or even no provisions and often no *Osmia* eggs. Because nests with the smaller 7.9 mm U-shaped tunnels were not made and set out until later in the spring, only a few were occupied. In these, the *Osmia* cell lengths were more consistent (13–14 mm). We do not know where this bee nests when trap nests are unavailable. Therefore, it is impossible to speculate on the meaning of the nesting patterns that are seemingly dictated by shape of the tunnels in artificial trap nests or why females expend effort in building and provisioning cells in a nest where eggs are not to be deposited. However, we wonder whether the peculiar nest of *O. caerulescens* with odd-shaped cells built into a large cavity and pictured by Malyshev (1935: fig. 67) may relate to the same phenomenon and whether offering either species a variety of semirestricted enclosures might be a way of exploring this phenomenon.

PROVISIONING: We found females of *Osmia chalybea* visiting only flowers of a purple-flowered thistle (*Cirsium horridulum* Michx.), although we made no effort to investigate sources of provisions. Other members of *Helicosmia* visit a wide range of plants (Hurd, 1979), so this species may well have similar habits. However, at our sites, all nests seemed to have been provisioned with pale pollen of uniform size and of one spherical, spiny morphology, suggesting a single plant source.

Stored fresh provisions tended to be dry pollen on the outer surface next to the cell wall and cell rear but were moist on the front surface, where the *Osmia* egg was inserted. When broken apart with forceps, provisions tended to be stratified in cross section suggesting that when one or more pollen loads were packed against the rear of the cell, the female may then have disgorged nectar on the then front surface before bringing another load of dry pollen. After doing this a sufficient number of times, the provisions reached completion, ready for egg deposition. The front surface of the completed food mass was always uneven, often with an irregular lump to one side and with the periphery extending farther forward than the central area of the front. The central area appeared darker, presumably wetted by nectar that the female had placed on it. Females invariably deposit eggs with the rear end buried in the provisions toward one side of the central area while the anterior end extended forward from the provisions (fig. 7).

DEVELOPMENT: *Osmia chalybea* has five larval instars. The first is almost certainly routinely pharate under the egg chorion. Although we were unable to identify head capsules and mandibles from cast skins, spiracles and a band of spicules that extended just above the spiracular line were visible on cast skins that were retrieved from a number of preserved specimens. Furthermore, we retrieved a preserved specimen (figs. 8–10) with the chorion partly removed, perhaps by the sloshing of the preservative. When viewed with an SEM, we were able to see the apically bidentate mandibles (fig. 8) and a band of sharp-pointed spicules extending just above the spiracles along the side of the body (figs. 9, 10). This combination of features has been used to identify the eclosion method of a number of other taxa (Alves-dos-Santos et al., 2002; Rozen et al., 2006; Rozen and Kamel, 2007; Rozen et al., 2010a).

We suspect that the first instar does not feed on pollen based on our previous experience with pharate first instars (as cited above), but we were unable to make observations on this matter here. Torchio (1989a) presented details of embryogenesis for three other species of *Osmia* that seem to closely correspond to our more casual observations. We assume that the second instar commences feeding on the provisions, and food is easily seen in its midgut. As a second instar, the anterior part of the larva's body bends toward the provisions, and its head comes in contact with the food while its posterior end remains attached to the provisions where the egg had been deposited. Subsequent instars retain this posture up to the time of the fifth larval stadium. Although we did not monitor developmental timing,



FIGURES 8–10. SEM micrographs of first instar of *Osmia chalybea*, with chorion partly removed, allowing examination of details. **8.** Front of head showing labrum, bidentate mandibles **9.** Spicules above spiracular line; note narrow and presumably misshapen atrial opening (dorsum of body segment toward upper right). **10.** Close-up of sharp-pointed spicules identified by rectangle in fig. 9.

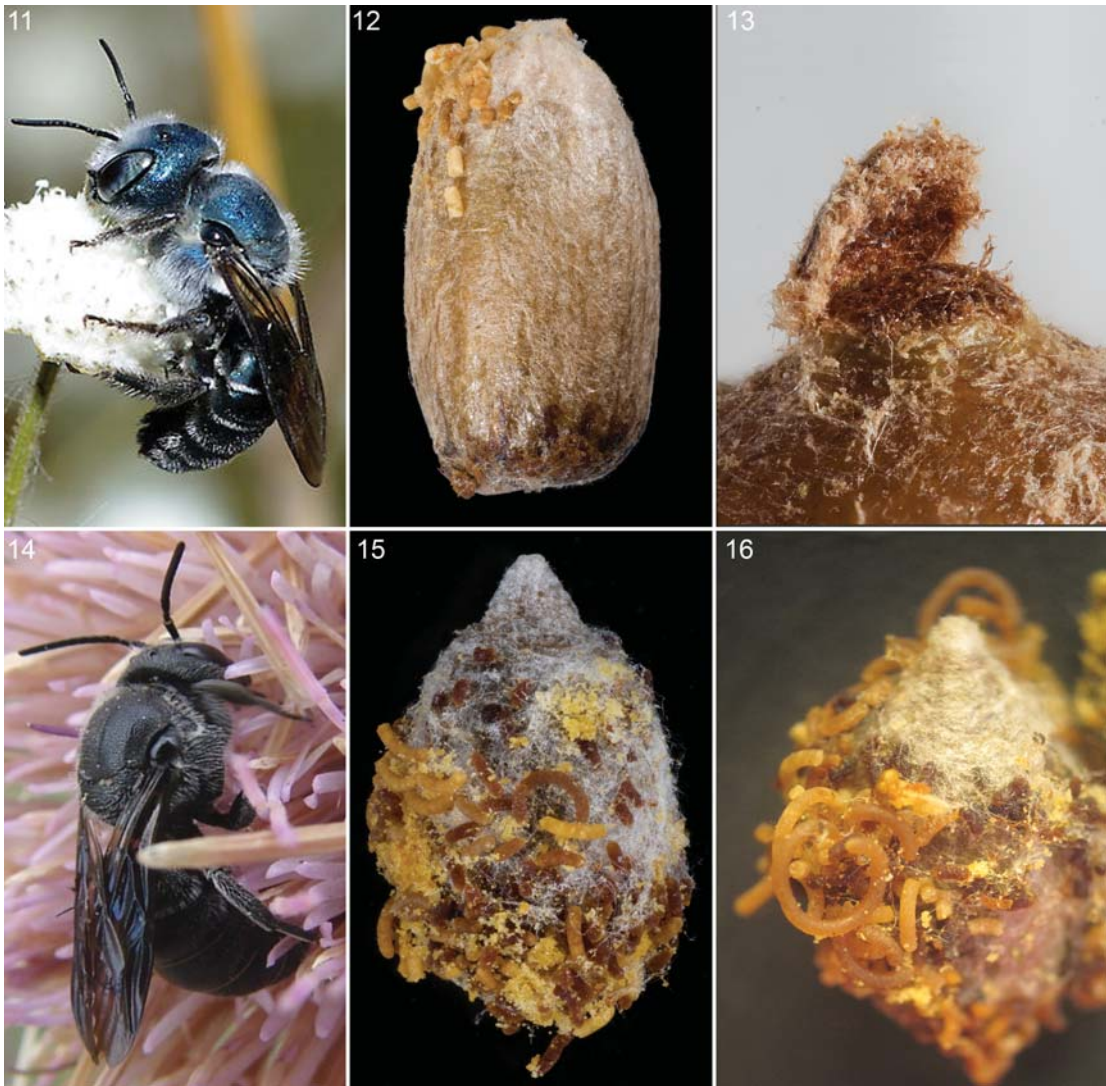
feeding larvae reach the last larval instar within a matter of days, well before most of the provisions are consumed. In two cases, we observed a newly emerged last larval instar on its food mass with approximately 80% of the food yet to be eaten. Not surprisingly, the fresh last larval instar is substantially smaller than the fully fed one but can be easily recognized because of abundant body setae (as is also the case for *Stelis ater*, fig. 87), which are not found on fourth and earlier instars.

Throughout the first four larval stadia, the connection between the mesenteron and proctodaeum remains closed, so that ingested food accumulates in the mesenteron. When the fifth instar sheds the previous exoskeleton, the connection opens and a small amount of fecal material is shed with the fourth-instar exoskeleton. Thereafter the newly emerged fifth instar of *Osmia chalybea* (as well as of *Stelis ater*) commences defecation. Both a filled proctodaeum and body setae signify fifth instars.

Defecation continues while provisions are consumed, and fecal pellets accumulate as a loose mass toward the front end of the cell opposite the stored food. The pellets at first tend to be mostly pale, more or less parallel sided, 2–5 (but mostly 3–4) times as long as their diameter, and often more or less truncated at both ends (note fecal pellets attached to cocoon, fig. 12). While still defecating, the larva starts spinning silk and eventually walls off much of the loose mass of previously deposited feces. New feces gradually become medium dark brown and are deposited at the rear of the cell and along the sides of the tunnel where they are enmeshed in the outer strands of the cocoon. The feces on the sides of the cocoon tend to be flattened, presumably by compression of the large, active larval body, and are deposited parallel to the long axis of the cocoon. Toward the end of defecation, the pellets become smaller, very dark, and more tapering at both ends.

COCOON: Cocoon structure in nests with U-shaped channels is difficult to study because of lack of uniformity of chamber shape and inconsistency of larval orientation. Therefore, cocoons from circle-shaped tunnels were primarily used in the following analysis. These cocoons were parallel to the long axis of the tunnel, their front facing the tunnel entrance. Completed cocoons (fig. 12) are tan externally with an outer layer of fine, nearly white silk in which are enmeshed fecal pellets. This layer occasionally adheres to the wooden wall of the tunnel where the diameter of the cocoon is widest rather than to the cocoon itself when the cocoon is removed. Pale feces deposited earlier at the front of the cell loosely surround the nipple end of the cocoon (described below), which is covered by a dense mass of cottony, nearly white, fine silk. At the rear of the cocoon, a large number of darker fecal pellets are incorporated mostly into the outer layer of the cocoon. Cocoon dimensions are about 7 mm maximum width and 12 mm long.

The paleness of the cocoon is created by the whiteness of fine loose fibers on the outer surface. Beneath the outer fibers a consistently tough, semitransparent leathery layer of somewhat darker material gives the finished cocoon most of its strength. Initially we thought that it was composed of many sheets of mostly fused silk, but on being boiled in an aqueous solution of sodium hydroxide, it became gelatinous, whereas silk fibers did not, suggesting that its source and chemical composition are different. An innermost thin layer of satiny, white, tissue-



FIGURES 11–13. *Osmia chalybea*. **11.** Photograph of adult female. **12.** Microptic photograph of cocoon, front end up, lateral view. **13.** Close-up of nipple of same with outer cocoon layer removed and cap pried up to show outer screen beneath, near lateral view. FIGURES 14–16. *Stelis ater*. **14.** Photograph of adult female. **15.** Microptic photograph of entire cocoon, front end up, lateral view. **16.** Microphotograph of same, showing characteristic elongate fecal pellets, lateral view.

like silk (fig. 18) is loosely attached by fine strands to as much as the front two-thirds of the cocoon but sometimes as little as only the front one-quarter. The inner surface of the rear part of the cocoon remains shiny and semitransparent through which streaks of fecal deposits are visible (figs. 18, 20). Although this whitish, tissuelike layer appears fenestrated, SEM examination (fig. 29) proves that it is an unbroken surface; the apparent dark areas are merely transparent areas of fused silk and the white areas are the fiber strands that connect this inner cocoon

layer to the middle layer seen through the fused silk. SEM images (figs. 27, 29) show no feature that distinguishes the inner surface of the front part of the cocoon from the rear part except at the nipple end. Hence, the thin, white, tissuelike inner layer fuses with the tough, semiopaque middle layer toward the rear of the cocoon. The only opening of the inner surface of the entire cocoon is at the nipplelike projection (figs. 27, 28, 30–32).

In cocoon descriptions of other bees (e.g., Rozen and Jacobson, 1980; Rozen and Buchmann, 1990), structures on cocoon front ends have been regarded as passageways permitting exchange of gases between the outside atmosphere and the inside of the cocoon, usually through a circular, screened aperture in the fabric that presumably excludes mites and/or other parasites/parasitoids from access to the developing bee within. The screening of the aperture is formed by crisscrossing of partly fused strands of silk. In the case of

Osmia chalybea, when the whitish cottony mass of silk is removed from the outer surface at the anterior end of the cocoon, the sharply projecting and seemingly truncate nipple area is revealed (figs. 13, 17). Not only does it project about 1 mm from the leathery middle layer of the cocoon fabric, it also expands apically into a broad, hard, slightly domed, externally fibrous brown cap, about 2.5 mm in diameter, which can be pried free with forceps to reveal beneath a circular surface (figs. 13, 17, 24) about 1.5 mm in diameter of coarse, twisted, interlocking, often reddish-brown fibers, forming the outer screen. Immediately behind this screen is a mass of compressed white fibers that stretch across the front end of the cocoon. Imbedded in these fibers is a thin, usually hard, whitish, semitransparent, plasticlike disc (figs. 17, 26) somewhat less than 1.0 mm in diameter. This disc is surrounded at its periphery as well as in front and behind by fine white fibers. Some variability exists among cocoons in the amount of these white fibers in the nipple. The inner lining of the cocoon lies behind this disc and surrounding fibers (fig. 17). The only place where there is an open passageway between the nipple and the inner lumen of the cocoon is either a screened circular opening (the inner screen) of the inner lining of the cocoon (figs. 19, 27, 28) at the nipple end or a number of small, less well-organized fenestrations in the same area (figs. 30–32).

We interpret the nipple end to be a filter area, allowing gas exchange between inside and outside of the cocoon and simultaneously protecting the larva/pupa within from invasion by parasites/parasitoids and predators, as follows. The fine, dense white silk that covers the outside

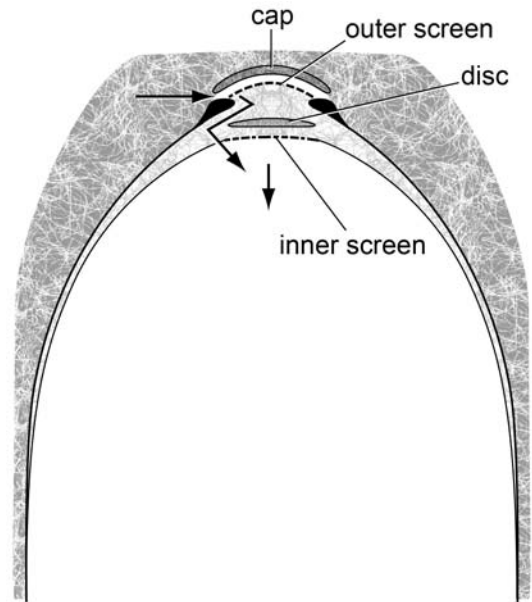
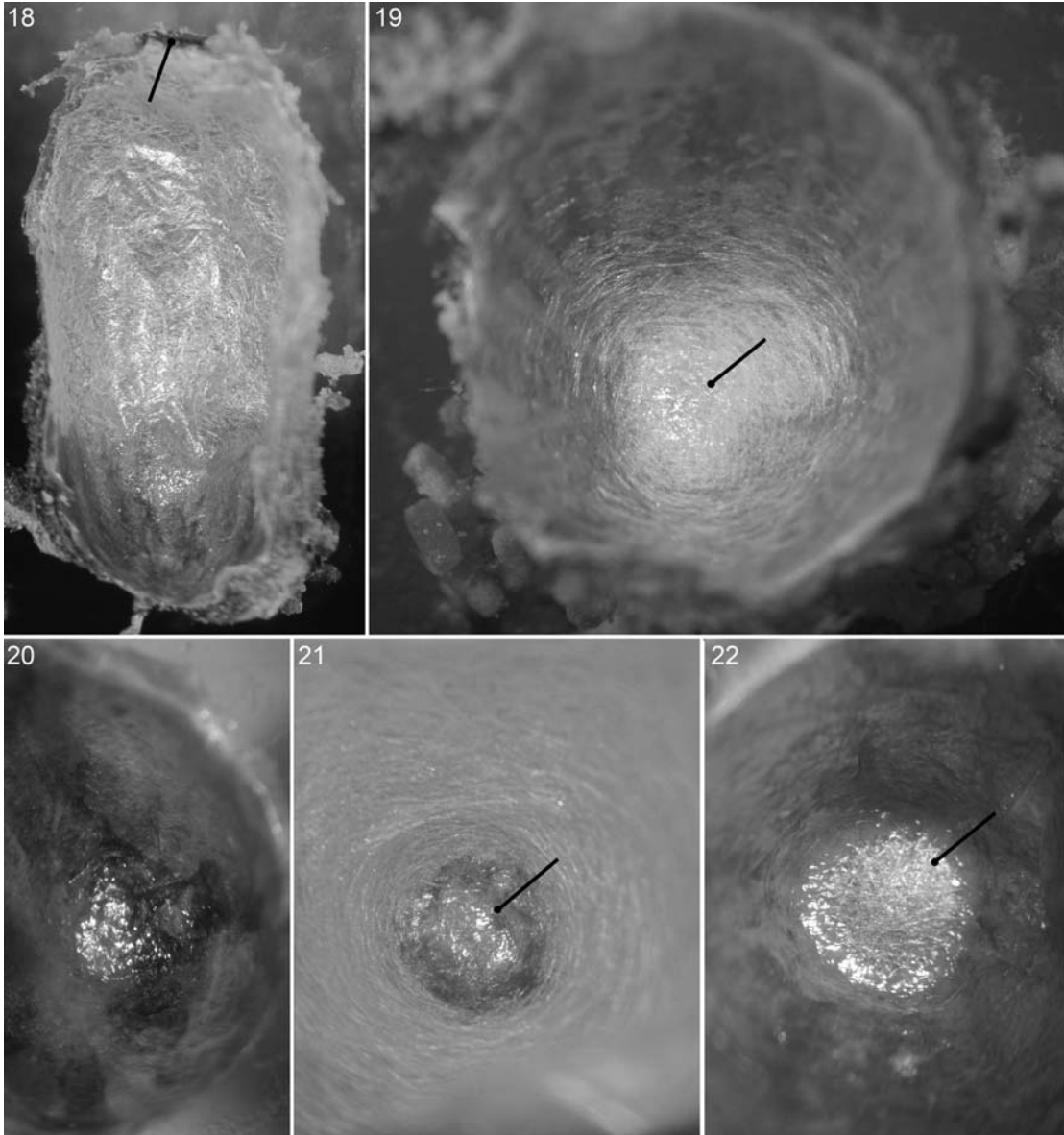
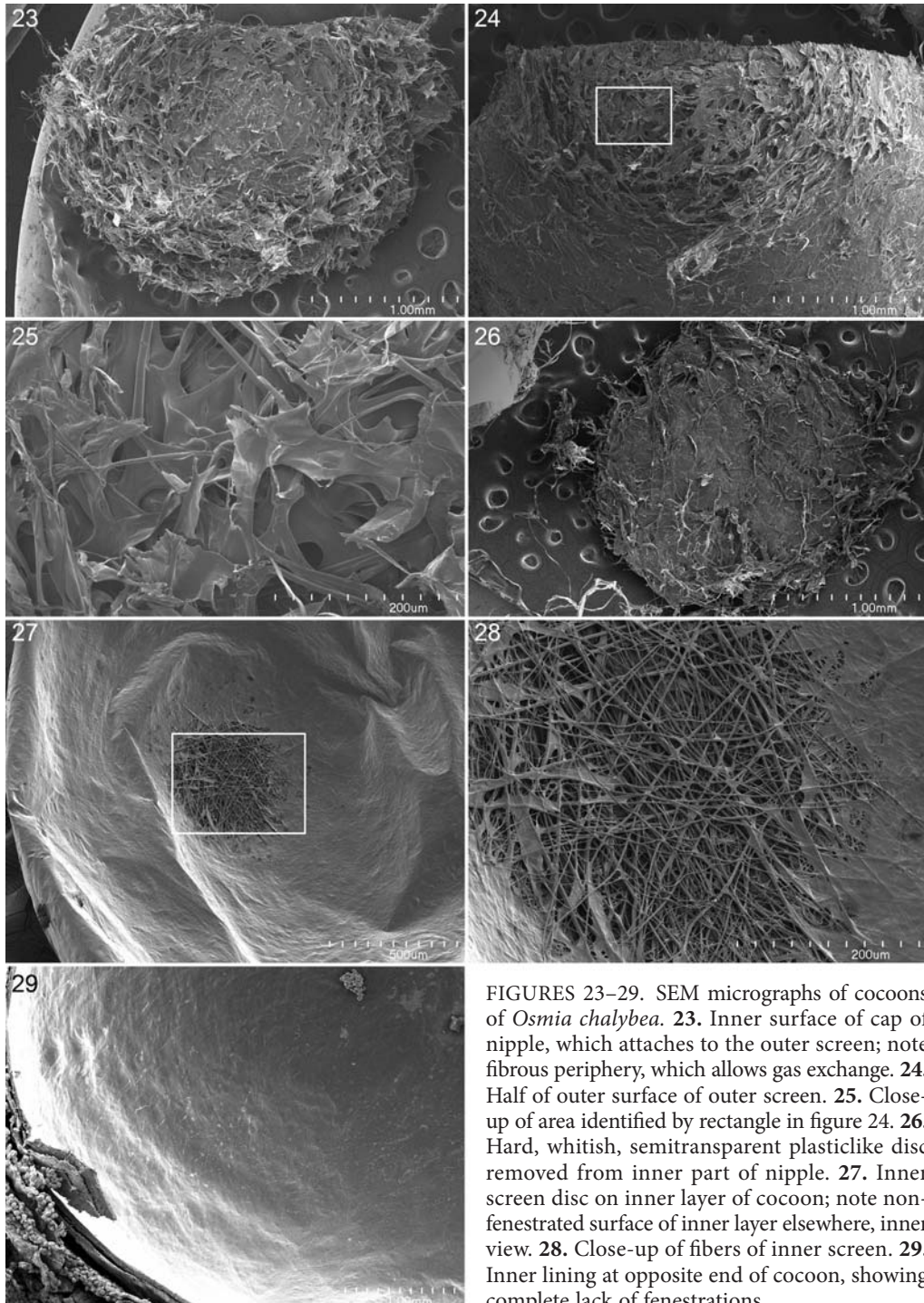


FIGURE 17. Diagram of front end of a cocoon of *Osmia chalybea*, showing elements of filter areas, side view, with arrows pointing direction of inflow air through filtered gas-exchange system of nipple.



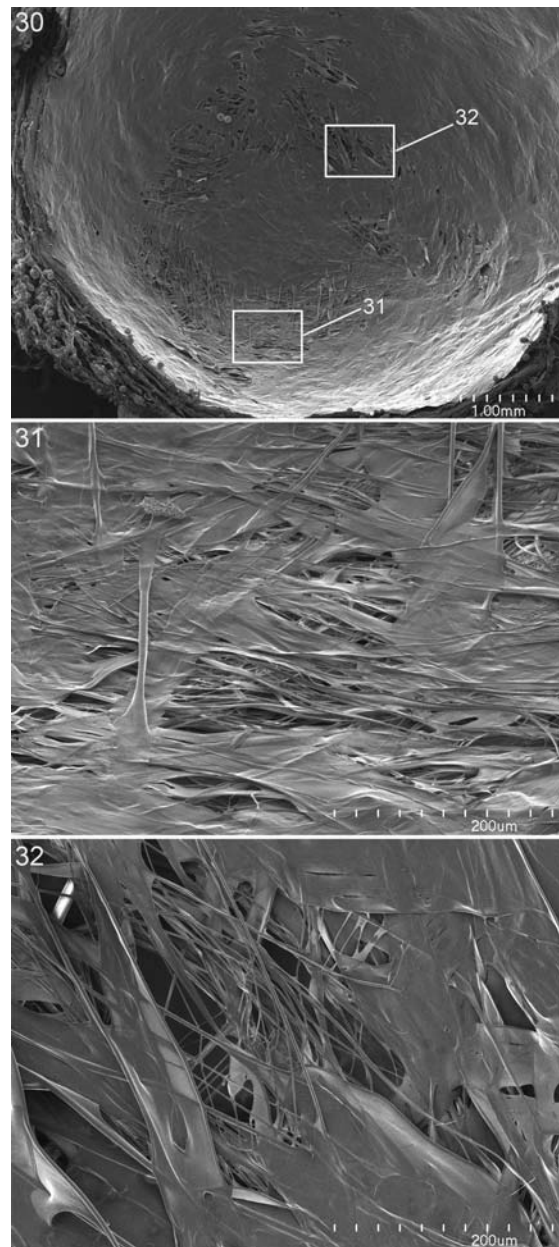
FIGURES 18–22. Microphotographs of cocoons of *Osmia chalybea*. **18.** Inner surface of cocoon with cap of filter removed, cut longitudinally, showing white inner layer on anterior section fusing posteriorly with middle layer to produce dark semitransparent surface; note dark outer screen of nipple (pointer). **19.** Front end viewed from inside, showing white silk of inner lining and inner screen (pointer). **20.** Rear end viewed from inside, showing shiny, semitransparent inner surface with fecal streaks. **21.** Front end of cocoon in early stages of construction viewed from inside, showing deposit of silk (pointer) that will make up hard cap of completed cocoon. **22.** Front end of cocoon before inner lining applied, viewed from inside, showing undersurface of outer screen (pointer) before turning dark.



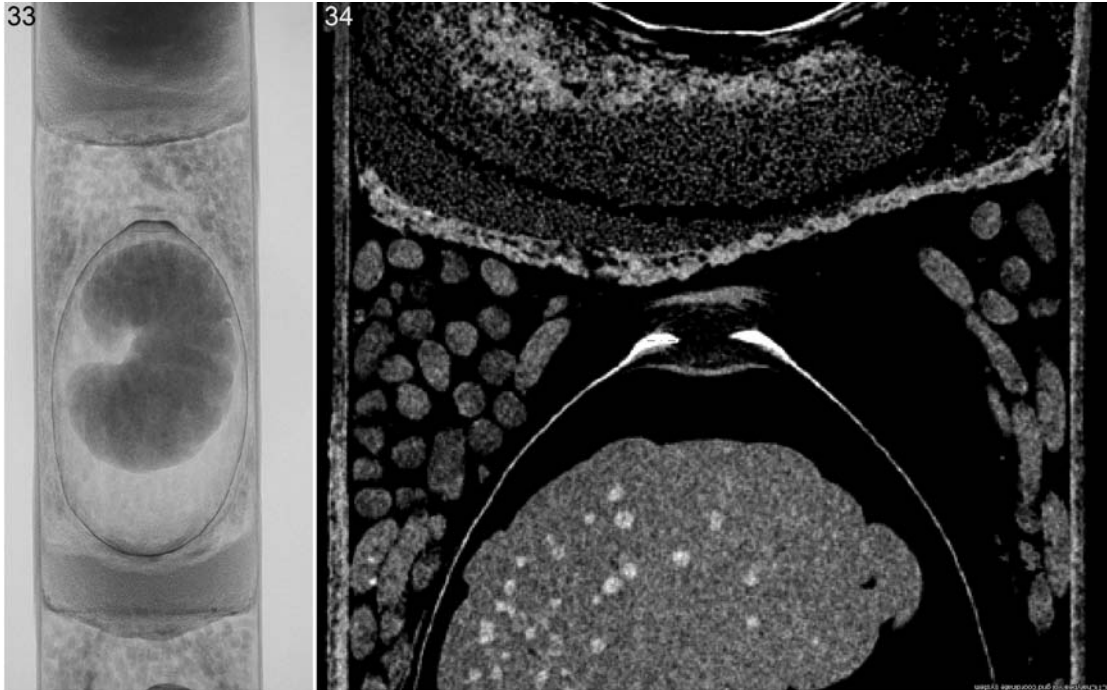
FIGURES 23–29. SEM micrographs of cocoons of *Osmia chalybea*. **23.** Inner surface of cap of nipple, which attaches to the outer screen; note fibrous periphery, which allows gas exchange. **24.** Half of outer surface of outer screen. **25.** Close-up of area identified by rectangle in figure 24. **26.** Hard, whitish, semitransparent plasticlike disc removed from inner part of nipple. **27.** Inner screen disc on inner layer of cocoon; note non-fenestrated surface of inner layer elsewhere, inner view. **28.** Close-up of fibers of inner screen. **29.** Inner lining at opposite end of cocoon, showing complete lack of fenestrations.

of the front end of the cocoon is probably a strong barrier to parasites, parasitoids, and predators, as seems to be the case for the dense white silk surrounding the entrance of the inner lining of the cocoon. We assume that the hard outer cap provides protection because of its resistance to penetration and because it narrows the passageway to the interior, which is also the case with the hard white disc in the filter itself. Under this scenario (arrows, fig. 17), outside air diffuses in through the periphery of the hard cap where the cap attaches to the rest of the nipple, then through the outer reddish screen and around the white inner disc, and then through the screened aperture of the inner cocoon lining. Carbon dioxide-laden air, of course, diffuses out the same route from the opposite direction. A study currently underway (Rozen, Rozen, and Hall, in prep.) confirms that the diffusion rate through the posterior half of a cocoon of *Osmia chalybea* is remarkably far less than through the anterior half of the cocoon bearing the nipple. Data from the study also indicate that the posterior portion exhibits an extremely low gas diffusion rate in absolute terms. This exceptional degree of impermeability would also assist the developing bee to avoid water loss.

Obviously a larva constructs its cocoon from the outside inward. Fine loose webbing is first attached to the brood chamber wall, and then strands of silk are deposited to form the beginning of the walls and front end of the cocoon. The inner shape of the front end of the cocoon is a curved surface with a narrower invagination centrally, the precursor to the nipple. The larva then deposits a shiny reddish mass (fig. 21) presumably of silk at the front end of this invagination, which



FIGURES 30–32. SEM micrographs of cocoons of *Osmia chalybea* viewed from inside. **30.** Inner screen of another cocoon in which the fenestrations are not in a disclike cluster. **31, 32.** Close-ups of fenestrations identified in fig. 30.



FIGURES 33, 34. Radiographs of cocoons of *Osmia chalybea*, side view. **33.** X-rayed cell containing mature larva surrounded by its cocoon. **34.** Slice of CT scan of another cocoon showing anterior end of cocoon close to rear of preceding cell; note components of filter system at nipple although fine, loose silk not visible.

fuses with the strands there and hardens to become the cap to the nipple. The larva then adds the other features to the nipple end. We were unable to determine when these features were added in relation to construction of the rest of the cocoon. We assume that the white plasticlike inner disc of the closure is formed in a similar manner to the cap, although why one is dark and opaque and the other pale and semitransparent is not apparent.

Cocoon spinning by three individuals reared at room temperature took about one week. A larva in a fully formed cocoon no longer contains feces and thus is uniformly yellowish (with no internal dark masses to be seen through the integument) except for the usual darkly pigmented integumental areas on the head. It is normally motionless, but when touched with a probe, its body rapidly curls and then uncurls by snapping its anterior end straight. As a result the head travels much of the length of the cocoon while its mandibles energetically open and close through two to four rapid cycles of curling and uncurling before the larva suddenly becomes motionless again. When in motion, the body slowly spins in the cocoon, so its head traverses a large area of the cell wall. When the larva is curled, its mandibles seem to groom its venter. This behavior continues even a month after completing the cocoon; there is no complete diapause. Such actions seem to be a defense tactic against predators, parasitoids, or parasites. Torchio in reviewing this manuscript stated: "Some *Hoplitis* and other *Osmia*, especially *O. (Helicosmia) texana* [Cresson] larvae, also curl and then snap the body to the straight posi-

tion.” He had observed a case in which a larval chrysidid brushed against a larva of *O. dimidiata* Morawitz in a cocoon. When the bee larva snapped its body, the chrysidid fell, and, when the bee larva snapped a second time, the chrysidid was crushed against the side of the cocoon. Paradoxically, these actions are far more vigorous when the *Osmia* larva is completely encased in a protective leathery cocoon compared with anytime before it is so confined, including when attacked by the fifth instar of *Stelis ater* (fig. 41)! See the following section.

The duration of larval feeding and development is brief. In three nests with U-shaped tunnels sent to J.G.R. on April 19, 2010, 31 surviving larvae of *Osmia chalybea* had spun cocoons and only three had not yet started by May 19, 2010. The same trap nests contained 3 cocoons of *Stelis ater* and 6 live larvae that had not yet started cocoon construction, suggesting cleptoparasite development is not racing with that of the host. This limited sample of surviving hosts and parasites (34:9) demonstrates a 21% cell parasitism rate.

Thirteen cocoons of *Osmia chalybea* that were opened on September 8–10, 2010, contained live pupae, 10 of which were females and 3 males, in various stages of pigmentation, from nearly all white to fully pigmented. No larvae were found. These data indicate that individuals of this species overwinter as adults, to emerge the following spring. The pupae were generally inactive and nonresponsive to being handled; none seemed capable of rotating its metasoma to alter its position in its cocoon. A single male, about to emerge, was capable of actively moving its legs and mandibles.

PARASITES: The minute native parasitoid wasp *Melittobia digitata* Dahms (Eulophidae) penetrated the cocoons and attacked larvae and pupae of *Megachile* Latreille (Hall and Ascher, 2010) and other aculeate Hymenoptera that began to use our trap nests later in the spring. *Melittobia* has a very broad host range (Krombein, 1967; Matthews et al., 2009) and may pose a serious threat to *Osmia chalybea* immatures, especially to those in the same trap nests with cells of some other species infested by *Melittobia*. However, *O. chalybea* seems to have several defenses, because the parasitoid wasps were not found in cells left intact or when first removed from the nests. The preferred hosts of *Melittobia* (i.e., apoid wasps and *Megachile*) nest later than *O. chalybea*. By the time the parasitoid wasps were observed, *Osmia* nesting was largely complete, and thereafter the parasitoid wasps may have been effectively excluded by the hardened leaf tissue that the bees use to seal and close their nests. If this material becomes broken, allowing *Melittobia* to enter, the cocoons would be another barrier. After being removed from the nests, *Osmia* and *Stelis* cocoons attracted *Melittobia* that had emerged from infested *Megachile* and *Trypoxylon* cells present in the same room. The parasitoid wasps succeeded in making small holes in the outer silk layer of the cocoons, but for more than a month their entry appeared to be blocked by the hardened middle layer. After two months, however, 3 out of 40 *Osmia* cocoons and 9 out of 21 *Stelis* cocoons had been penetrated. Previously, we had found that *Melittobia* larvae developed successfully on both *Osmia* and *Stelis* larvae exposed after cutting off parts of the cocoons. When wasps first landed, *Osmia*, but not *Stelis*, larvae responded with rapid curling and uncurling motions, driving the wasps away. After a couple of hours, the *Osmia* larvae had been overcome by wasps and had become immotile, perhaps paralyzed by the wasps' stings (Matthews et al., 2009). In unopened cocoons, these larval movements may

be more effective repelling, or perhaps even killing, wasps that must enter one at a time through their small holes.

Our observations were similar to those of Balfour[-]Browne (1922) studying *Melittobia acasta* Walker. *Osmia rufa* L. was among potential hosts investigated. Adult *Melittobia* present on the bee larvae were killed by its cocoon-spinning motions. Thereafter, the completed cocoons were too hard to be penetrated by wasps. *O. rufa* appeared to have an additional defense. Although the *Melittobia* oviposited on bee larvae removed from their cocoons, the majority of the wasp brood feeding on the larvae died.

No other cleptoparasitic bees were seen entering or attacking nests of *Osmia chalybea*. However, collected adults of *O. chalybea* carried sometimes abundant phoretic deutonymphs of the mite *Chaetodactylus rozeni* Klimov and O'Connor (kindly identified by Pavel B. Klimov). According to Klimov and O'Connor (2008) members of this genus "when possible, kill the bee egg or larva in its early developmental instar and then feed on the provisioned food inside the cell." However, we observed no evidence that they attack early stages of *O. chalybea*. The only other bee known to transport this mite is the related *O. (Helicosmia) georgica* Cresson (ibid.).

BIOLOGY OF *STELIS ATER*

EGG DEPOSITION: We discovered eggs of *Stelis ater* on the front surface of the provisions and others deeply buried in the provisions. Because we detected no mechanism whereby eggs could have been inserted after cell closure, we assume that they are introduced only into cells that have yet to be closed by the host female, as also reported for other *Stelis* by Torchio (1989b). It is unclear how the eggs are buried since there are no special modifications at the end of the female metasoma of this species that would assist in inserting the eggs deeply. A likely possibility is that all eggs are deposited on the existing exposed surface of provisions and, if the provisions are incomplete, deposited eggs are buried when foraging host females return to add more larval food. However, this assumption needs confirmation, because in other cases of bee cleptoparasitism, we think that returning host females search out and destroy cleptoparasite eggs. It seems unreasonable that *Osmia chalybea* females would not do so.

According to observations by P.H. Torchio (personal commun., October 25, 2010), *Stelis montana* appears to modify its egg laying behavior to match that of its host. When parasitizing *Osmia (Cephalosmia) californica* Cresson and *O. (Cephalosmia) montana* Cresson, it constructs an egg chamber within the provisions, as do those hosts. However, when parasitizing *O. (Osmia) lignaria* Say, it lays its egg on the surface of the provisions, as does that host. He commented that all three *Osmia* species and *Stelis montana* attach their eggs to provisions only by their posterior ends, and they all begin feeding as second instars.

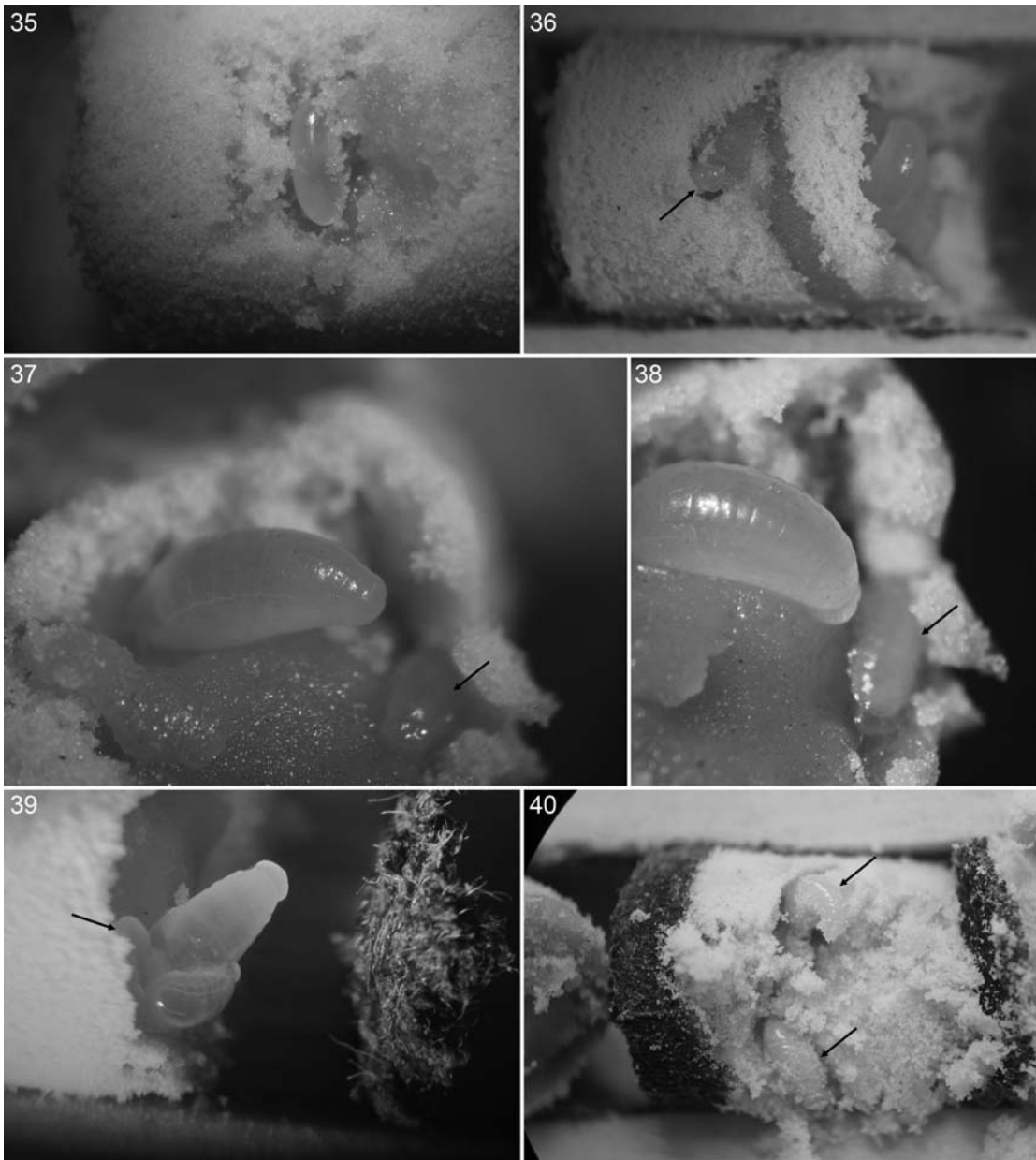
DEVELOPMENT: *Stelis ater*, like its host and *S. montana* (Torchio, 1989b), has five larval instars evident from accumulated cast skins. We assume that the first is pharate because of the lack of sclerotization of its head capsule and because mandibles were not detected on any first instar skins, although spiracles were. Although we did not find a band of spicules above the spiracular line on each side of the body of first instars, we would not be surprised if future studies identified such bands; we simply had insufficient material.

J.G.R. had anticipated that the last larval instar would be found to be the prime hospicidal stage because of the extreme modification its head capsule and mouthparts as found in figures 83–85, 95, and 96. However, our study of this species clearly indicates that most stages are capable and behaviorally inclined to attack host immatures and one another if they encounter them. Although most cells contained a single cleptoparasite, not uncommonly two occurred in a cell, and in two cases three cleptoparasitic larvae coexisted apart from one another in a cell. Figures 35–41 show various examples. This variability in timing of encountering host or competing cleptoparasitic larvae results from the diversity of where the parasite eggs are deposited in the provisions and the now-realized fact (elaborated in the Discussion) that early stage megachilid larvae are incapable of crawling from the position where the egg is deposited.

Hence, if a recently hatched cleptoparasite is far removed from the host immature, both it and the host will increase in size substantially before they meet. A case in point was the discovery of a fifth instar of *Stelis ater* feeding on the surface of the provisions while a fourth instar of *Osmia chalybea* fed alongside it. About an hour after discovering the two larvae feeding side by side, we returned to discover the fifth instar of *S. ater* repeatedly chewing into the side of the host larva, an activity that continued for more than 10 min. The attacking larva then fell away from its host but continued to defecate until preserved. The wound on the side of the host larva was large and obviously fatal (fig. 42). The host larva did not react in any way to the attack, suggesting it had no defense response to deflect or avoid its attacker. Examination of the provisions afterward revealed that the egg of the *S. ater* had been deposited deeply, close to the cell wall. The pathway to the surface was a channel in the provisions close to the cell wall extending to the surface of the provisions. Near the egg-insertion point the channel was narrow but gradually widened as it progressed forward to the surface. The cast larval skins of instars 1–4 were layered against one another, and the flattened mass was pressed against the channel wall. At the farthest rear of the channel, presumably where the egg had been deposited, were two fecal pellets associated with the posterior end of the larval exuviae. Because only last instars defecate, these two pellets indicated that the posterior end of the fifth instar had been positioned at the approximate point where the egg had been deposited. One of these fecal pellets was presumably encased in the posterior end of the cast-off exoskeleton on the fourth instar, suggesting that it was the meconial mass first extruded after the intima of the fourth instar's hindgut had been withdrawn from the fifth's alimentary tract, allowing passage of fecal material from the midgut to the exterior.

A similar attack occurred when we found a moderately small last larval instar of the host and a *Stelis ater* of similar stage feeding next to the cell wall in the provisions. We moved the cleptoparasite with forceps and placed it by the host, with the result that we were able to watch the attack involving the repeated opening and closing of sharp-pointed *Stelis* mandibles. On the other hand, figure 39 represents the situation where two *Stelis ater* eggs were presumably deposited on the surface of the provisions close to the host egg with the result that the two early cleptoparasitic instars attacked the young host larva almost immediately. Presumably the two attackers would then have battled one another had we not preserved them.

Motions of an attacking early instar are not particularly agile: They consist merely of a repeated but routine opening and closing of mandibles usually unaccompanied by a thrusting



FIGURES 35–40. Immatures of *Stelis ater*. **35.** Egg deep in provisions; eggs were encountered both in the provisions and on the front surface of the provisions, as discussed in text. **36.** Early instar (arrow) deep in the provisions and feeding larva of *Osmia chalybea* (right) on front surface of provisions. **37.** Egg of *Stelis ater* (arrow) and probable first instar of *Osmia chalybea* (left) on front surface of provisions with trachea now visible. **38.** Same cell some time later with *Stelis ater* (arrow) now early feeding instar having not yet encountered *Osmia chalybea*, which has become an intermediate instar. **39.** Early instar of *Osmia chalybea* being attacked simultaneously by two early instars of *Stelis ater*; one of which (arrow) is barely visible to the left of the others. Presumably one *S. ater* larva would later kill the other, since we never found more than one cocoon in a cell. **40.** Two feeding early instars of *Stelis ater* (arrows) from eggs deposited deep in provisions.

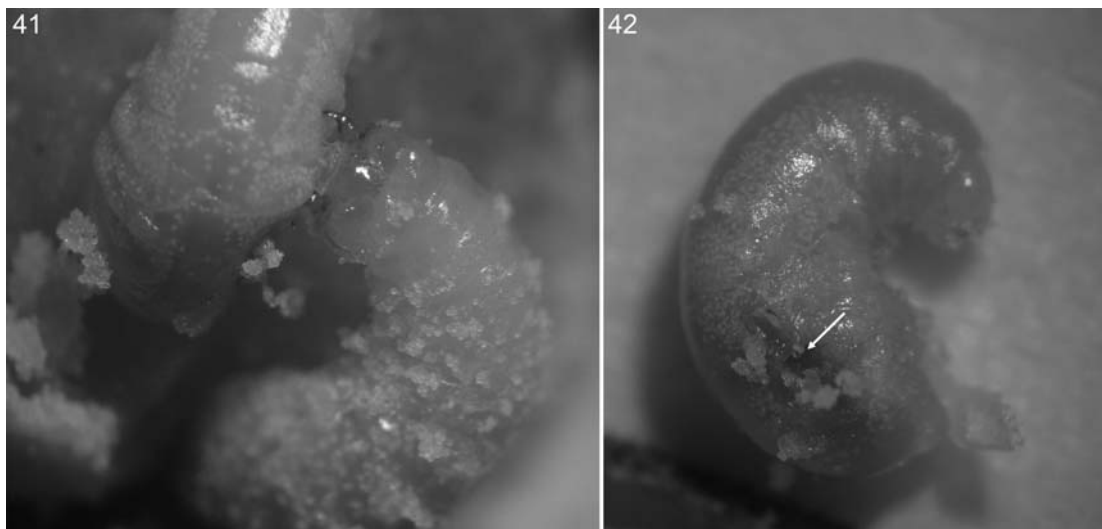


FIGURE 41. Early fifth instar of *Stelis ater* attacking fourth instar of *Osmia chalybea*. FIGURE 42. Wound (arrow) in same fourth instar caused by attack.

or turning head (although fig. 41 seems to be an exception). When a mandibular apex catches onto some part of the victim, this action is followed by continuing mandibular opening and closing until the victim is mortally damaged.

After becoming the fifth instar, the larva begins defecating, with the fecal material extruding slowly from the anus as a single, coiling, grayish-yellow strand, slightly more than 0.25 mm wide (fig. 14), in sharp contrast to the short cylindrical pellets of the host. The occurrence of such coils in a cell permits certain identification of *Stelis*, as Torchio (1989b) reported a similar phenomenon with respect to feces of *S. montana*. Of course, we do not know whether all species of *Stelis* produce such feces. As the larva increases in size, the strand often breaks into sections of irregular lengths though rarely as short as those of the host. By the time of cocoon spinning, feces have become very dark and more fusiform (note mixture of pale and dark feces in figs. 15, 16).

After cocoon spinning, the larva becomes totally quiescent, with its head end closest to the front end of the cocoon. Its flaccid body no longer responds to being touched by forceps or by being moved, unlike the host larva. *Stelis ater* is now in diapause. The first parasite

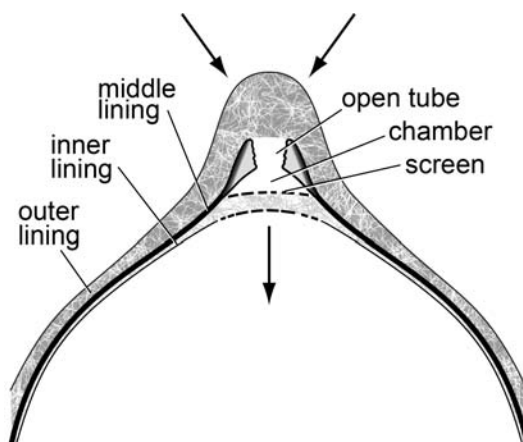
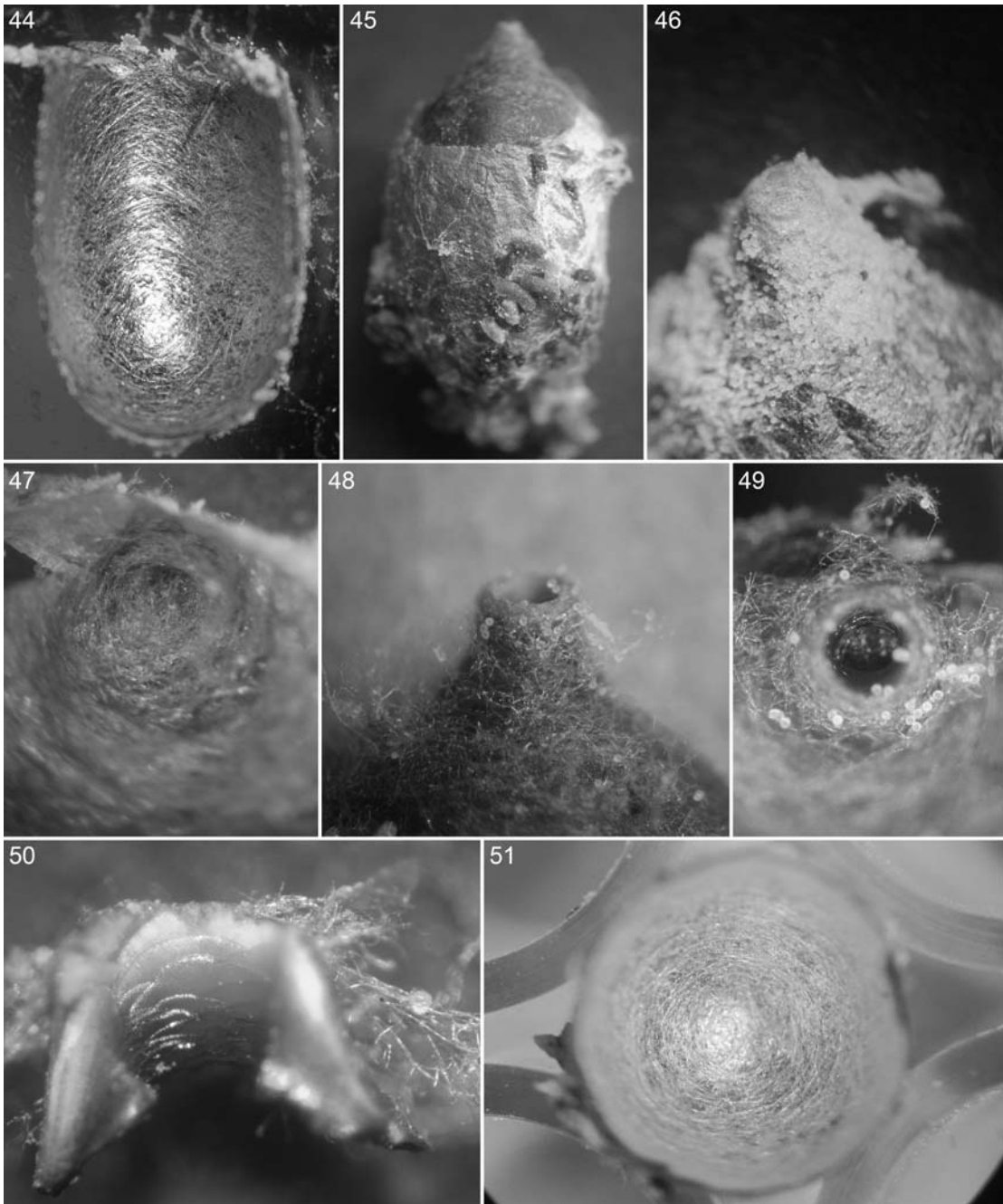


FIGURE 43. Diagram of front end of cocoon of *Stelis ater*, showing elements of filter area, side view, with arrows pointing direction of inflow air through filtered gas-exchange system of nipple.



FIGURES 44–51. Microphotographs of cocoons of *Stelis ater*. **44.** Inner surface of rear of cocoon cut longitudinally. **45.** Entire cocoon, with outer lining removed from front end, revealing nearly black inner surface of nipple and middle layer of cocoon, lateral view. **46.** Exterior surface of outer layer of nipple end, lateral view. **47.** Interior surface of outer layer of nipple showing mass of silk fibers that surrounds and covers passageway to interior. **48.** Inner layer of nipple with outer layer removed showing opening of passageway to rest of filter system, approximate lateral view. **49.** Front view of opening to inner layer showing open passageway to screen

pupa to emerge from a cocoon stored at ambient room temperature was preserved January 17, 2011, by which time almost all hosts had emerged as adults.

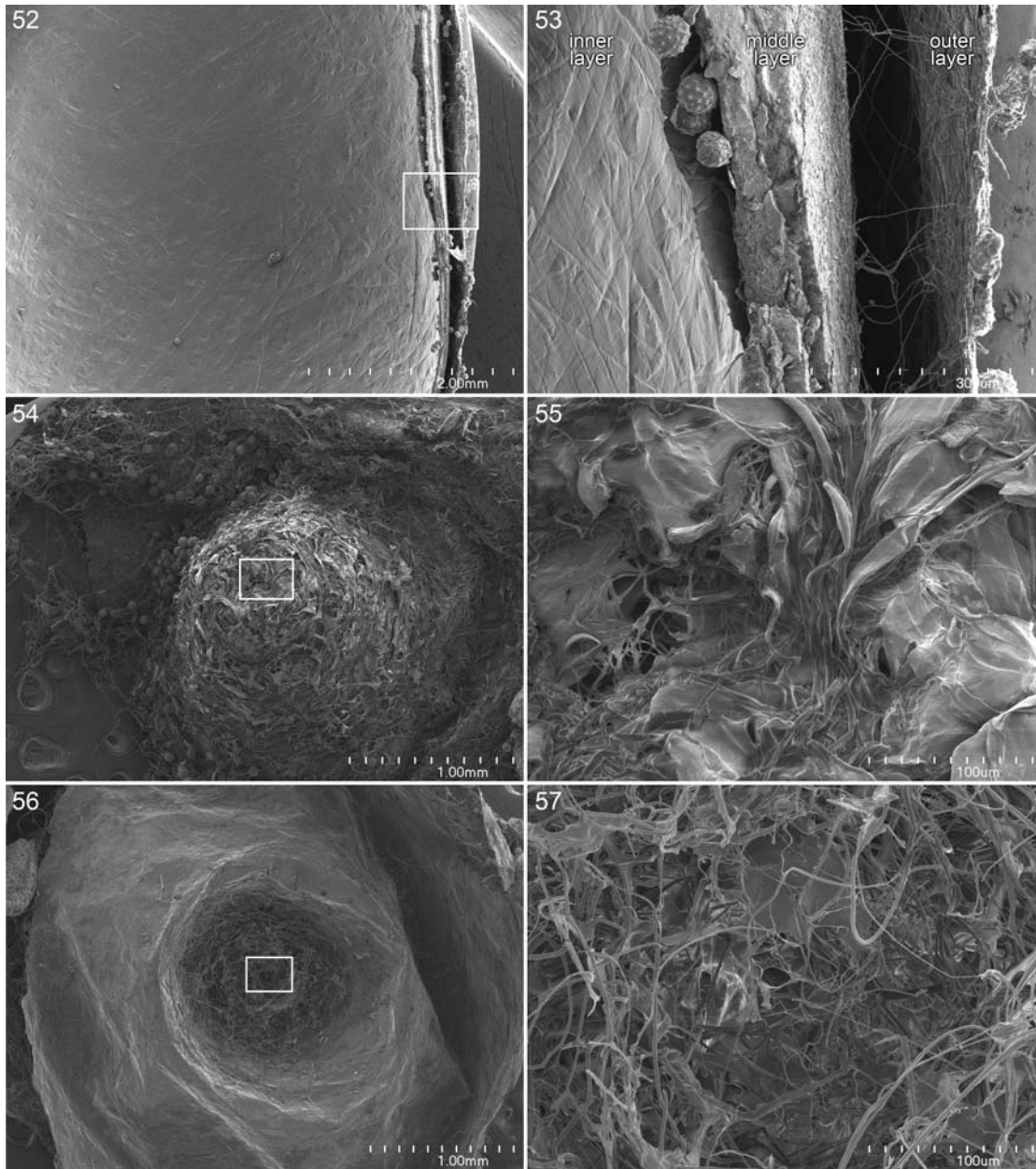
COCOON: Externally the cocoon of *Stelis ater* is similar to those of other species of *Stelis* that have been described or pictured (see Parker, 1986; Parker et al. 1987; Rozen and Kamel, 2009, and references therein). All are characterized by having the anterior end drawn out into an elongate, tapering nipple (figs. 15, 16, 43, 68–70). For *S. ater*, six cocoons in U-shaped tunnels were oriented with their long axis at about 45° from horizontal. All had their front ends pointed upward and all but one had the front ends pointed toward the tunnel entrances. The nipple is not hidden in a mass of fine silk as is the case with *Osmia chalybea*, although it has a thin surface covering of whitish strands. The body of the cocoon, but not its nipped front end (figs. 15, 16), is submerged in a mixture of uneaten pollen and fecal pellets loosely held together by strands of silk. Fecal pellets closest to the cocoon tend to be short and dark, as mention above. The cocoon is about 8.5–12 mm long and approximately 4.7–6 mm in maximum diameter (N = 4).

The fabric of the body of the cocoon consists of three distinct layers (figs. 43, 52, 53). The outer layer is a thin sheet of semitransparent grayish-tan silk, more or less covered by loose strands of white silk (fig. 15). This layer is loosely connected by tan strands to the thick, ridged middle layer, which is opaque, very dark brown to nearly black, leathery, and strongly resistant to compression. The source and composition of this layer was at first unknown, since silk fibers could not be detected in it. However, Torchio's (1989b) description of cocoon construction in *Stelis montana* almost certainly explains that the material comes from the larva's anus and is the excreta of the Malpighian tubules.³ The thin inner layer consists of shiny strands of silvery silk (fig. 44) when first deposited, that later sometimes become faintly coppery against the dark background of the middle layer.

The outer layer of the cocoon also covers the entire nipple, giving the nipple end its characteristic tapered appearance, with its length gradually narrowing to an acutely rounded, conical apex (figs. 15, 16). Viewed with an SEM, the fabric of the outer surface is dense but fenestrated (figs. 54, 55). Immediately under its apex is a dense mass of loose, pale tan silk fibers (figs. 56, 57) that surrounds and covers the apex of the strongly projecting middle layer of the cocoon that is continuous with the inner layer of the nipple. The latter is an externally dark, hollow tube (figs. 43, 48, 49, 58, 70), apically about 0.7 mm across and with a central circular opening about

³ This observation by Torchio (1986b) suggests that the dark substances combined with sand grains coating the inner surface of cocoons of *Fidelia villosa* Brauns (Rozen, 1970) and *Pararhophites orobinus* (Morawitz) (McGinley and Rozen, 1987), both in the basal clade of Megachilidae, may also be from Malpighian tubules. It is worth noting that not all *Stelis* cocoons have a middle layer that is opaque, dark brown to black: Parker et al. (1987) reported that cocoon fabric of *S. (Dolichostelis) rudbeckiarum* Cockerell was amber colored, "less dense and the overwintering prepupal larvae were visible" through it.

←
of filter area. **50.** Close-up of inner layer of nipple with one side removed showing pale cream color of silk and glassy surface, approximate lateral view. **51.** Anterior end of cocoon viewed from inside, showing white inner lining to cocoon.



FIGURES 52–57. SEM micrographs of cocoons of *Stelis ater*. **52.** Cross section of cocoon wall showing three layers. **53.** Close-up of area identified by rectangle in figure 52. Note non-fenestrated surface and thinness of inner layer in figs 52, 53. **54.** Exterior surface of outer layer of nipple removed from rest of cocoon showing nature of fabric. **55.** Close-up of area identified by rectangle in figure 54. **56.** Under surface of outer layer of nipple removed from cocoon showing dense fibers. **57.** Close-up of area identified by rectangle in figure 56, showing texture of fabric.

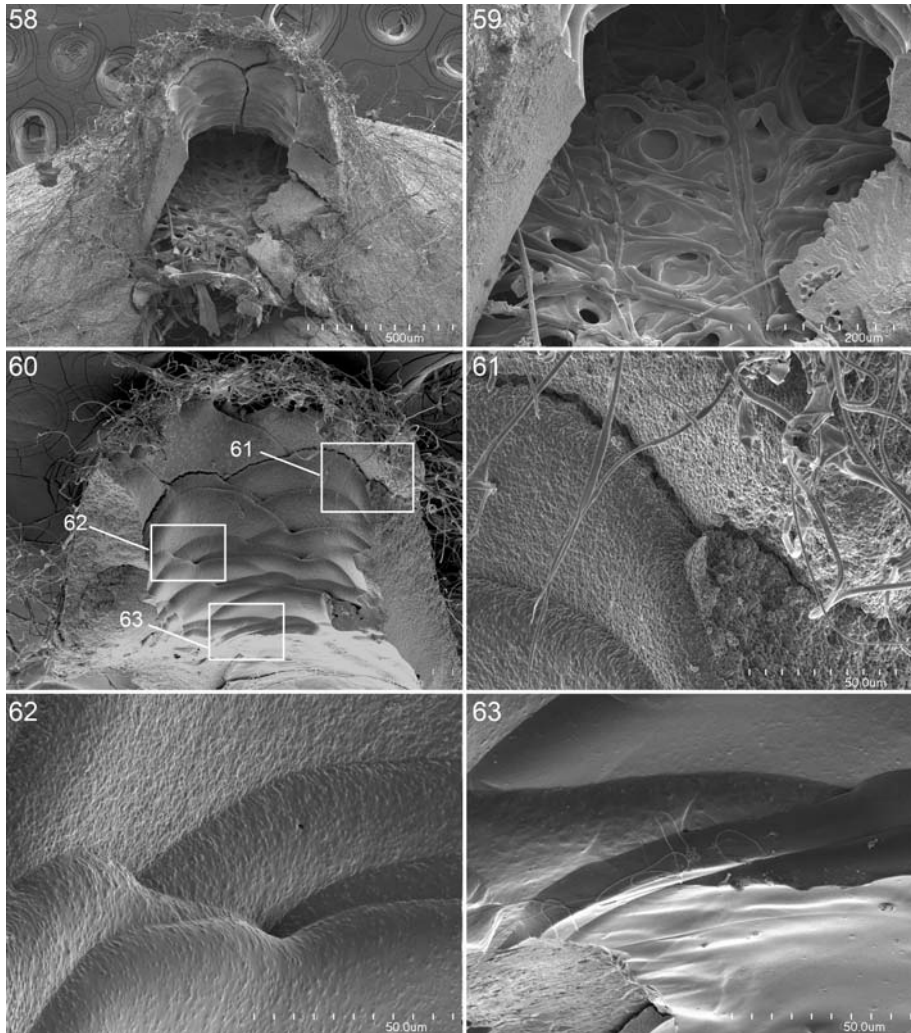
0.33 mm in diameter. This opening is the outer end of an open passageway leading to the interior of the cocoon. The tube is approximately 0.75 mm long. About halfway to the base of the tube, the passageway widens into an inner chamber about 1.0 mm in diameter at its base. Its base is covered with a disc of thick, reddish fibers that screens the passageway to the lumen of the cocoon (figs. 58, 60).

When the outer layer of the cocoon is removed, the middle layer is seen to connect flawlessly to the inner layer of the nipple externally (fig. 45). However, they are apparently made from two different materials. Whereas the middle layer of the cocoon wall is entirely blackish brown throughout, the inner layer of the nipple is dark only on the outer surface. Internally it pales to a creamy white toward its apex (fig. 50). Furthermore, its inner surface develops a glassy consistency with a transparent appearance (fig. 50). The ripplelike marks on the wall of the inner passageway of the nipple (figs. 50, 58, 60–63) suggest that it may be a glassy secretion of silk. This suggestion is reinforced by an earlier observation (seen in one of the observation nests) of a larva with its head moving inside the outer layer of the cocoon nipple, an unexplained behavior at the time. Exactly where the black material of the middle layer of the cocoon transforms into the glassy material of the nipple is difficult to identify because of the thinness of the cross section. Future observations of spinning larvae should be able to explain the phenomenon. Immediately behind the screen of the nipple is the inner layer of the cocoon wall with multiple small openings scarcely visible without an SEM (figs. 64, 65); it is present behind the nipple end but not elsewhere (fig. 66). Incoming air (fig. 43, arrows) obviously enters through the opening in the outer layer, then through the open passageway of the nipple, through the screen, and finally through the openings of the inner cocoon layer. Gas exchange takes place along the same route. The study by Rozen, Rozen, and Hall (in prep.) currently underway shows that the cocoon of *Stelis ater* is even more airtight than that of *Osmia chalybea*.

We think that the airtight nature of cocoons of both species is derived from the thin inner cocoon layer with openings through this layer only at the nipple end. If true, then the smooth surface to this layer as seen in the SEM micrographs (figs. 27, 29, 52, 56, and 66) is evidence of air tightness. Although our original assessment was that this surface is formed by fusion of silk strands, we cannot ignore the possibility that it is a composite material, i.e., some other secretion spread over a foundation of silk strands.

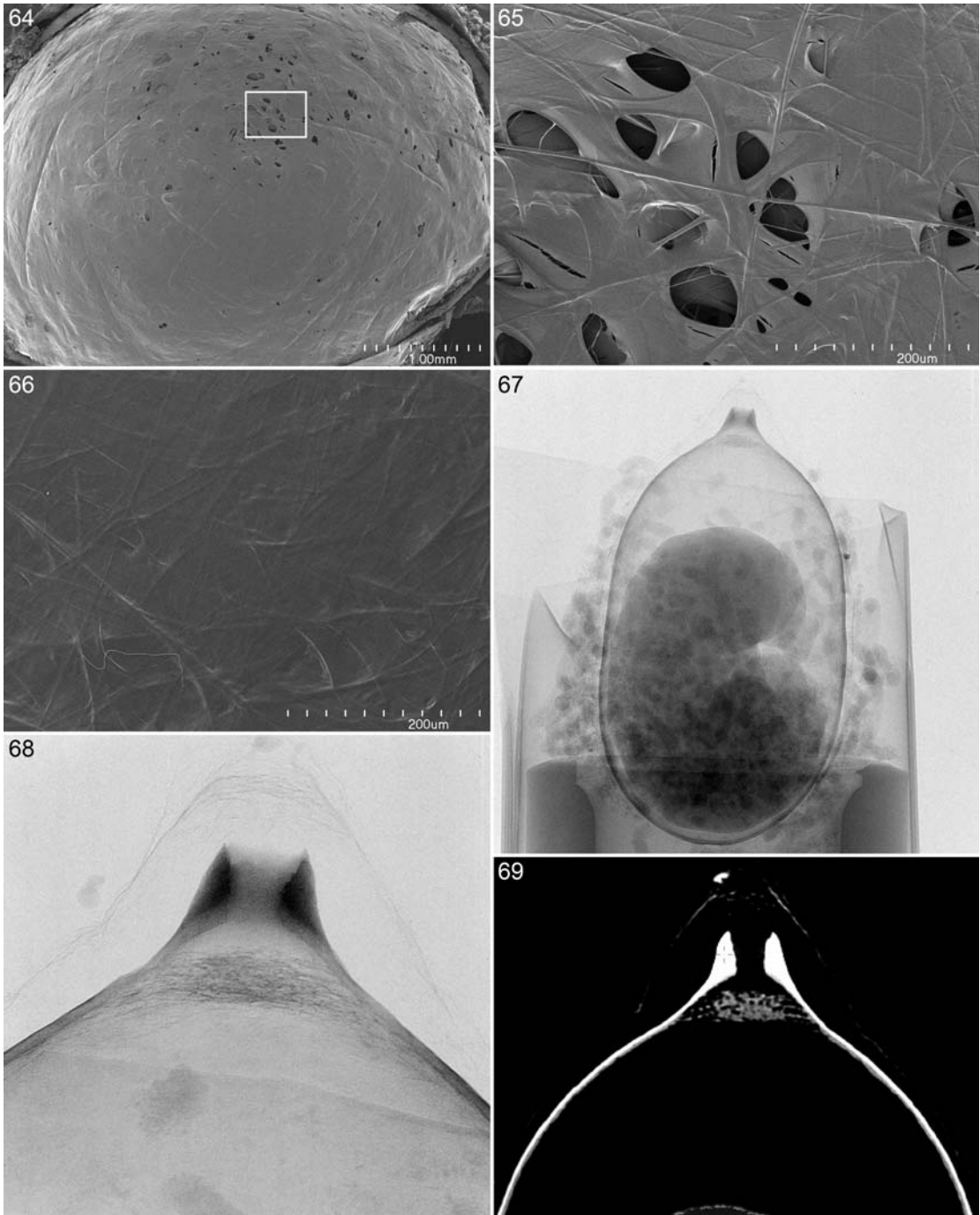
COMPARISON OF COCOONS: A comparison of the cocoons of *Osmia chalybea* (the host) and *Stelis ater* (the cleptoparasite) is of interest if for no other reason than we have often devoted little attention to the function and structure of bee cocoons,⁴ although there is a growing body of knowledge concerning the properties and use of silk by honey bees (*Apis mellifera* Linnaeus) (e.g., Sutherland et al., 2007, and references therein). It seems likely that the silk of *O. chalybea* and *S. ater* will be made of proteins in a coiled coil arrangement, as seems to be characteristic of aculeate Hymenoptera (Sutherland et al., 2007). In summary, cocoons of both species as

⁴ Contrary to this statement, Michener (1955) and Rust and Thorp (1973) provided rather detailed and thoughtful descriptions of the cocoons of *Stelis lateralis* and *S. chlorocyanea*, respectively, which seem in many ways comparable to our account of the cocoon of *S. ater*. However, without specimens to compare side by side, the differences cannot be evaluated and resolved.



FIGURES 58–63. SEM micrographs of nipple end of cocoon of *Stelis ater* with outer layer of cocoon removed. **58.** Part of nipple removed to expose passageway from tip of nipple to screened surface. **59.** Close-up of screen forming base of chamber. **60.** Part removed from nipple, showing texture of inner surface thought to result from larva pushing silk forward from inside the cocoon. **61–63.** Close-ups of area identified by rectangles in figure 61, respectively; note changes in surface texture of silk, with silk of inner chamber shiniest.

described above provide larvae with an environment that screens out deleterious parasites, parasitoids, and predators and that protects the larva from dehydration with a nearly airtight cocoon fitted with a filtering nipple end to allow for gas exchange. At the same time, the structures of the two cocoons, particularly of the filtering devices, are significantly different and demonstrate the versatility of silk and the diversity of behaviors of larvae of the two species in applying the material. SEM studies (e.g., Rozen and Buchmann, 1990) strongly hint that cocoons of other bee taxa, though structured differently, may well afford similar protection.



FIGURES 64–66. SEM micrographs of inner layer of *Stelis ater* cocoon. **64.** Front end showing opening behind nipple. **65.** Close-up of area identified by rectangle in figure 64. **66.** Rear of cocoon, to same scale as figure 65, showing lack of fenestrations. FIGURES 67–69. Radiographs of cocoon of *Stelis ater* with live larva, side view. **67.** Entire cocoon. **68.** Close-up of anterior end; for explanation, see text. **69.** Slice of CT-scan anterior end.

DISCUSSION: There would appear to a selective disadvantage for a megachiline cleptoparasitic bee to have a host larva feeding on provisions that the cleptoparasite needs for survival. This problem was first implied when Baker (1971) correctly identified the third instar of several species of *Coelioxys* to be the chief hospicial stage. J.G.R. in a study of *Stelis elongativentris* Parker (Rozen, 1987) found that even the fifth instar was equipped to kill the large *Ashmeadiella* host larva. Recently, larvae of *C. chichimeca* Cockerell were discovered with their posterior ends attached to the egg insertion point until they reached the fourth instar (Rozen et al., 2010a). The only known hospicial first instars of cleptoparasites in the family are those that emerge from eggs deposited on host eggs, i.e., *Radoszkowskiana rufiventris* (Spinola) (Rozen and Kamel, 2007) and *C. (Allocoelioxys) afra* (Ferton, 1896) and *C. coturnix* Pérez (Rozen and Kamel, 2008). We propose that the underlying reason is that earlier instars of the cleptoparasites cannot reach their host because of an inability to crawl. Examination of non-cleptoparasitic Megachilinae (if not all Megachilidae) reveals that their early instars also lack that ability. Note the sessile posture of *Osmia chalybea* until it reaches the last larval instar (35, 36).

To the extent known, all Megachilidae spin cocoons; these structures may also afford protection from desiccation and parasite/parasitoid invasion. However, cocoon spinning is not a universal behavior of bees. Indeed, no other family consists solely of cocoon-producing species, and in two families (Stenotritidae and Andrenidae), no cocoon spinners have been reported. Future biological investigations should consider the mechanisms by which noncocoon spinners cope with brood parasitism/predation and desiccation.

OVARIAN STATISTICS OF *OSMIA CHALYBEA* AND *STELIS ATER*

Three individuals of *Osmia chalybea* and five of *Stelis ater* each had three ovarioles per ovary. Only one individual of *O. chalybea* clearly had a mature oocyte. Two individuals of *S. ater* had mature oocytes; one had two mature oocytes and the other had three mature oocytes. By dividing the length of the oocyte by the distance between the outer rims of the tegulae of the female from which they came, the single female of *O. chalybea* had an egg index of 0.72, and the two females of *S. ater* had an average egg index of 0.59 (see Iwata and Sakagami, 1966).

These data are compared with information from several recent studies dealing with these two genera in table 1. The egg index of *Osmia chalybea* is essentially the same as that of *O.*

TABLE 1. Ovarian and Mature Oocyte Statistics for Species of *Osmia* and *Stelis*

Taxon	Egg index	Total mature oocytes per specimen	Mature oocytes per ovariole	Ovariole formula	No. of specimens	References
<i>Osmia submicans</i>	0.71	1.25	0.21	3:3	4	Rozen and Kamel, 2009
<i>Osmia chalybea</i>	0.72	1	0.17	3:3	1	Current study
<i>Stelis elongativentris</i>	0.61	2.67	0.44	3:3	3	Alexander and Rozen, 1987
<i>Stelis murina</i>	0.64	2	0.33	3:3	6	Rozen and Kamel, 2009
<i>Stelis ater</i>	0.59	2.5	0.42	3:3	2	Current study

(*Pyrosmia*) *submicans* Morawitz, both of which are among the lowest values known for the genus (ibid.: table 1; Rozen et al., 2010b). So far, all *Osmia* indices fall into the *small* and *medium* categories of Iwata and Sakagami (1966: table 2). The only values for *Stelis* are those in table 1, although Iwata and Sakagami (1966) calculated that of the related *Euaspsis basalis* Ritsema to be 0.53, close to the figures for *Stelis* and all categorized as *small*.

IMMATURE STAGES OF *OSMIA CHALYBEA* AND *STELIS ATER*

OSMIA CHALYBEA

EGG/MATURE OOCYTE

Figures 7, 70, 71, 73–75

DESCRIPTION: Egg length 3.2–3.58 mm; maximum width 1.1–1.3 mm (N = 5); mature oocytes length 3.0 mm; maximum diameter 1.1 mm. Shape slightly curved with ventral surface weakly concave in lateral view; anterior end broadly to narrowly rounded in lateral view; posterior end also variably rounded; maximum breadth posterior to midbody (figs. 71, 72); micropyle a cluster of pores (figs. 74–76) surrounded by faint converging lines on normally curved surface of front of egg near anterior pole, not visible under stereomicroscope. Egg color translucent whitish; chorion under stereoscope clear, shiny, glassy. Under SEM examination chorion featureless except for micropylar area.

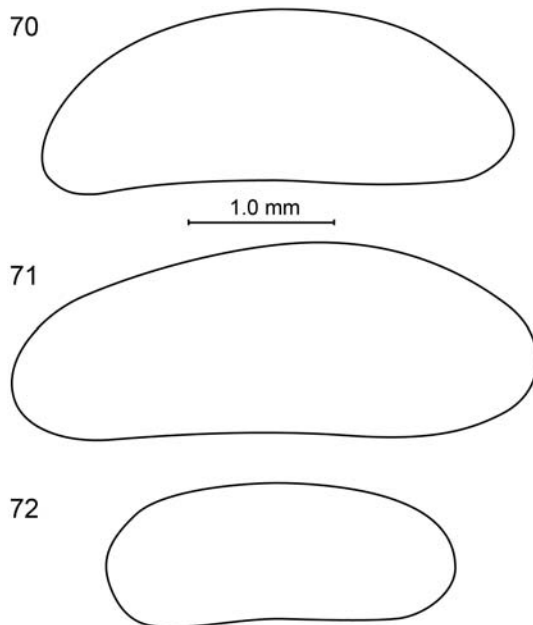
FIFTH INSTAR

Figures 79–81, 91

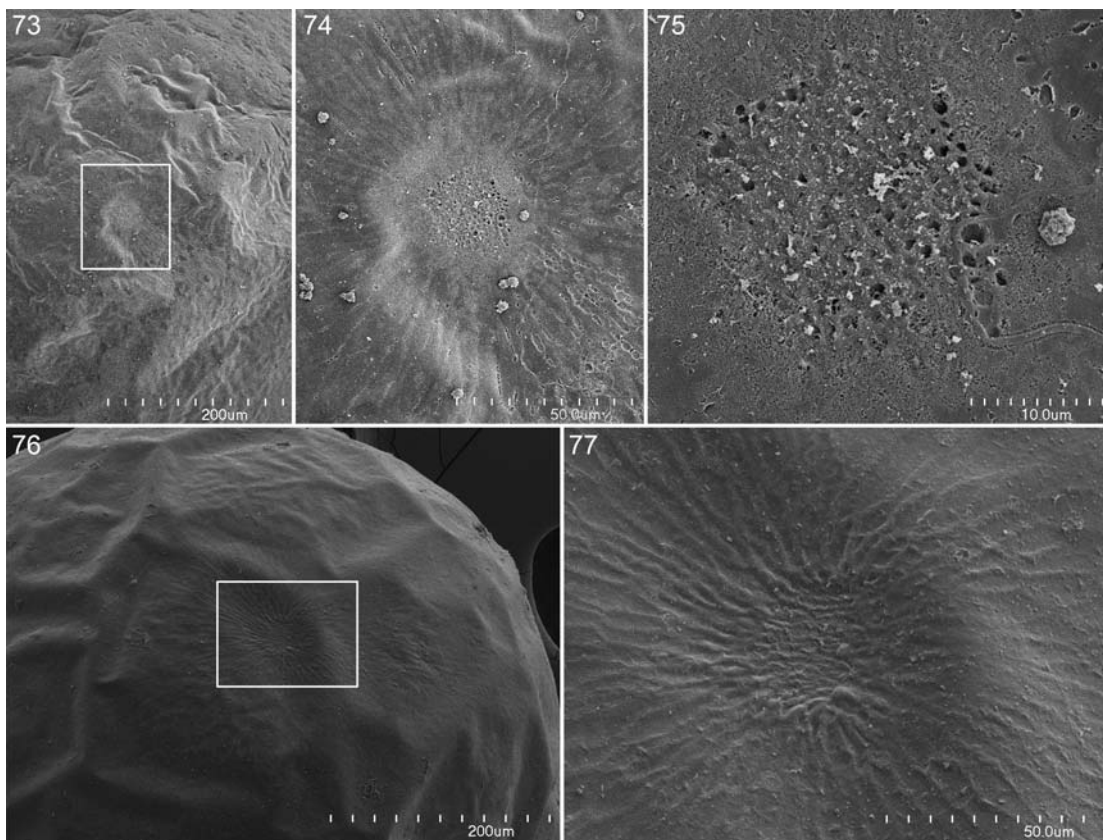
The following is based on both defecating and postdefecating forms.

DIAGNOSIS: The last larval instar of *Osmia chalybea* is remarkably similar to the recently described larva of *O. (Ozbekosmia) avosetta* Warncke (Rozen et al., 2010b). They can be distinguished in that the length of antennal papilla of *O. avosetta* is three times its basal diameter and the dorsal apical edge of the dorsal mandibular tooth is crenulate (ibid.: figs. 35, 36), whereas in *O. chalybea* the length of the antennal papilla is less than twice its basal diameter and the dorsal apical edge of the upper mandibular tooth is completely smooth (fig. 91).

DESCRIPTION: Head (figs. 81, 91): Setae long and abundant; those of frons shorter



FIGURES 70–72. Diagrams of eggs of *Osmia chalybea* (70, 71) and *Stelis ater* (72), lateral view, anterior end toward left, all to same scale; two diagrams of *O. chalybea* demonstrate variation in shape possibly a result of different ages of embryos.



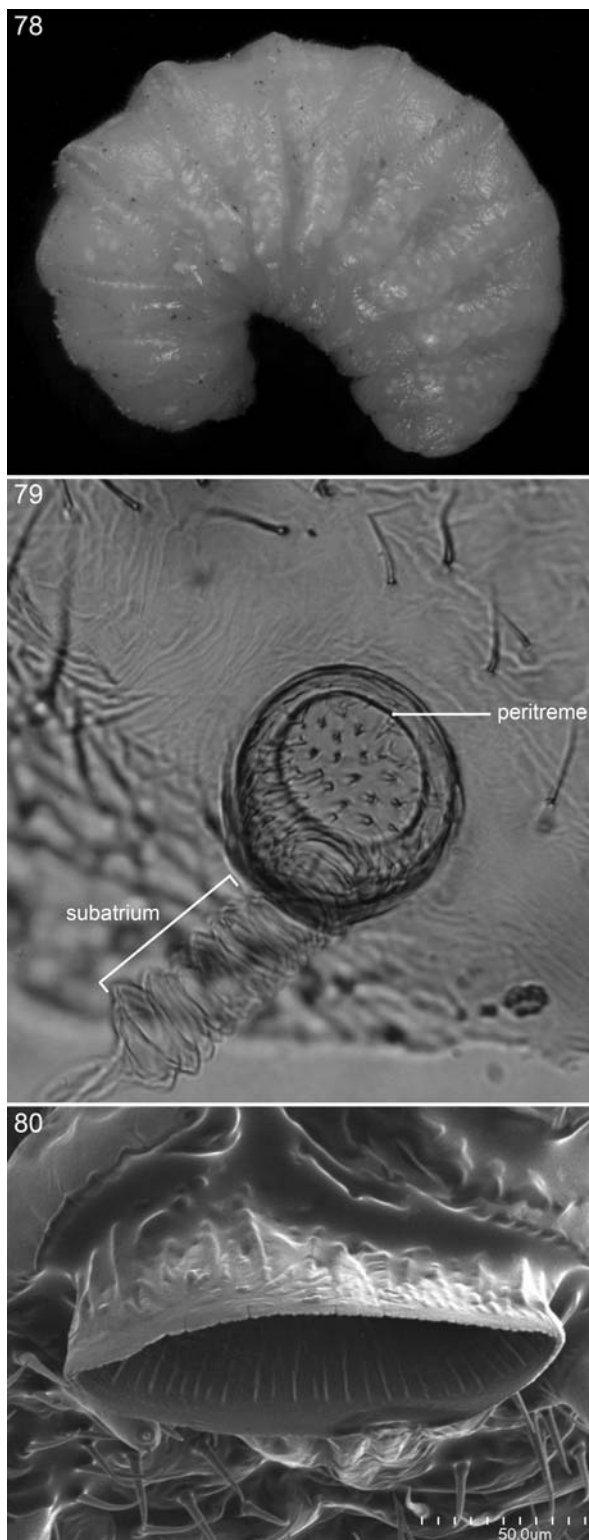
FIGURES 73–77. SEM micrograph of anterior ends of eggs of *Osmia chalybea* and *Stelis ater*. 73. Anterior pole of egg of *O. chalybea*. 74. Micropylar area of same identified by rectangle in figure 73. 75. Close-up of micropylar disc of same. 76. Anterior pole of *Stelis ater*. 77. Micropylar area of same identified by rectangle in figure 76.

and those of labrum very short; those of maxillary and labial apices straight, forward projecting. Head pigmentation generally weak (further weakened by clearing with aqueous solution of sodium hydroxide); following areas pigmented: labrum including labral sclerite and area distad of it; hypostomal ridge; mandibular apex and points of articulation; internal head ridges at articulation with mandibles; following sclerites faintly pigmented: cardo; stipital rod and sclerotized apex and articulating arm of stipes; premental sclerite; antennal papilla and all palpi. Fine spiculation restricted to lateral surface of paired hypopharyngeal lobes. Area immediately above hypostomal ridge and just behind posterior mandibular articulation not produced as downward-directed tubercle as present in many *Coelioxys* (Rozen and Kamel, 2007: fig. 47). Coronal ridge short, nearly absent; postoccipital ridge well developed; when viewed from above, ridge bending forward from each side, so juncture at midline obtusely angled; hypostomal ridge well developed, giving rise to pronounced dorsal ramus that extends posteriad from middle of ridge nearly to postoccipital ridge where it abruptly stops; anterior tentorial pit approximately equally distant from anterior mandibular articulation and basal ring

of antenna; epistomal ridge present only laterad of anterior tentorial pits; tentorium robust including dorsal arms. Parietal bands faintly evident. Antennal papilla small, length somewhat less than twice basal diameter, bearing two to three sensilla. Lower margin of clypeus strongly angled upward at midline, so that at midpoint margin approximately at level of anterior tentorial pits. Labral sclerite transverse, faintly to moderately pigmented; labrum lacking darkly pigmented median spot extending from labral sclerite to apical labral margin as in fully pigmented *Coelioxys* larvae (Rozen and Kamel, 2007: figs. 44, 45); apical labral margin moderately broadly emarginated in postdefecating form to deeply emarginated in some defecating larvae (probably an indication of soft, pliable texture of labral apex).

Mandible (fig. 90) moderately robust; apex bidentate with ventral tooth longer than dorsal tooth; both teeth acutely pointed; dorsal apical edge of dorsal tooth smooth; ventral apical edge of upper tooth and both edges of ventral tooth unmodified; apical concavity pronounced, sharply defined basally; cuspal area not produced; outer surface with single basal seta. Cardo present as sclerite; stipital rod slender; articulating arm of stipes evident; maxillary palpus moderately slender, longer than antennal

FIGURES 78–80. Last larval instar of *Osmia chalybea*. **78.** Macroptic photograph of entire larva, lateral view. **79.** Microphotograph of spiracle showing spined atrial wall, peritreme, and nearly parallel-sided subatrium. **80.** SEM micrograph of salivary lips showing parallel ridges of inner surface of lower lip, frontal view.



papilla. Labium clearly divided into prementum and postmentum; apex normally wide; premental sclerite weakly sclerotized; postmentum nonsclerotized. Salivary lips projecting, transverse, width about equal to distance between bases of labial palpi. Hypopharynx consisting of two widely separated lateral lobes, lateral surfaces of which are spiculate.

Body (figs. 78): Body setae moderate in length, not rising from swollen bases as in *Osmia avosetta*, extremely abundant, even more so than in *O. avosetta*; pleural area of abdominal segment 8 with approximately 80 setae; integument with fine network of irregular polygons, without spicules. Body form robust; on defecating form intersegmental lines at most weakly incised and intrasegmental lines not evident; on postdefecating form intersegmental lines well incised on anterior part body, less so on posterior part and intrasegmental line well formed on anterior part but becoming less so posteriorly, not evident beyond abdominal segment 6; paired body tubercles absent; middorsal body tubercles evident on midbody segments of postdefecating larva; pleural swellings moderately developed; abdominal segment 10 short, attached to approximate middle of segment 9; anus positioned toward top of segment 10. Spiracles (fig. 79) well sclerotized, unpigmented, subequal in diameter; atrium globular with width somewhat greater than depth, projecting above body wall, apparently without rim; peritreme narrow, so diameter of atrial opening approximately four times peritreme width; atrial inner surface with fine, sharply pointed, concentrically directed spines; primary tracheal opening with collar; subatrium perhaps variable in length, with as many as 12 chambers; externally, subatrium approximately parallel sided with first and innermost chamber of equal width. Male and female sex characters unknown.

MATERIAL EXAMINED: Numerous postdefecating and defecating fifth instars preserved various times in April, May, and June, 2010.

STELIS ATER

EGG/MATURE OOCYTE

Figures 35, 73, 76, 77

DIAGNOSIS: Eggs/mature oocytes have been described for *Stelis elongativentris* (Rozen, 1987) and *S. (Stelis) murina* Pérez (Rozen and Kamel, 2009). Those of *S. ater* are remarkably similar in color and shape, all characterized by their shortness relative to maximum diameters, rounded front ends, and slightly more narrowly rounded posterior ends. Of the three species, those of *S. ater* are the longest.

Eggs of *Stelis ater* can be immediately distinguished from those of the host by shape and size. Those of *Osmia chalybea* are substantially longer, and their maximum diameter is posterior to midbody as seen in lateral view (figs. 70, 71) rather than at the midbody as in *S. ater* (fig. 72).

DESCRIPTION: Length 2.2–2.4 mm; maximum width 0.88–0.98 mm (N = 5) at approximate midbody. Shape slightly curved with ventral surface flat to slightly concave in lateral view; anterior end broadly rounded in lateral view; maximum breadth at midbody with posterior half tapering to slightly more narrowly round posterior end in lateral view (fig. 72); micropyle a disc (fig. 77) surrounded by converging ridges on normally curved surface of front of egg at

anterior pole (fig. 76) not visible under stereomicroscope; apparent absence of pores not understood. Egg color translucent whitish; chorion under stereoscope clear, shiny, glassy. Under SEM examination chorion featureless except for micropylar area.

FIFTH INSTAR

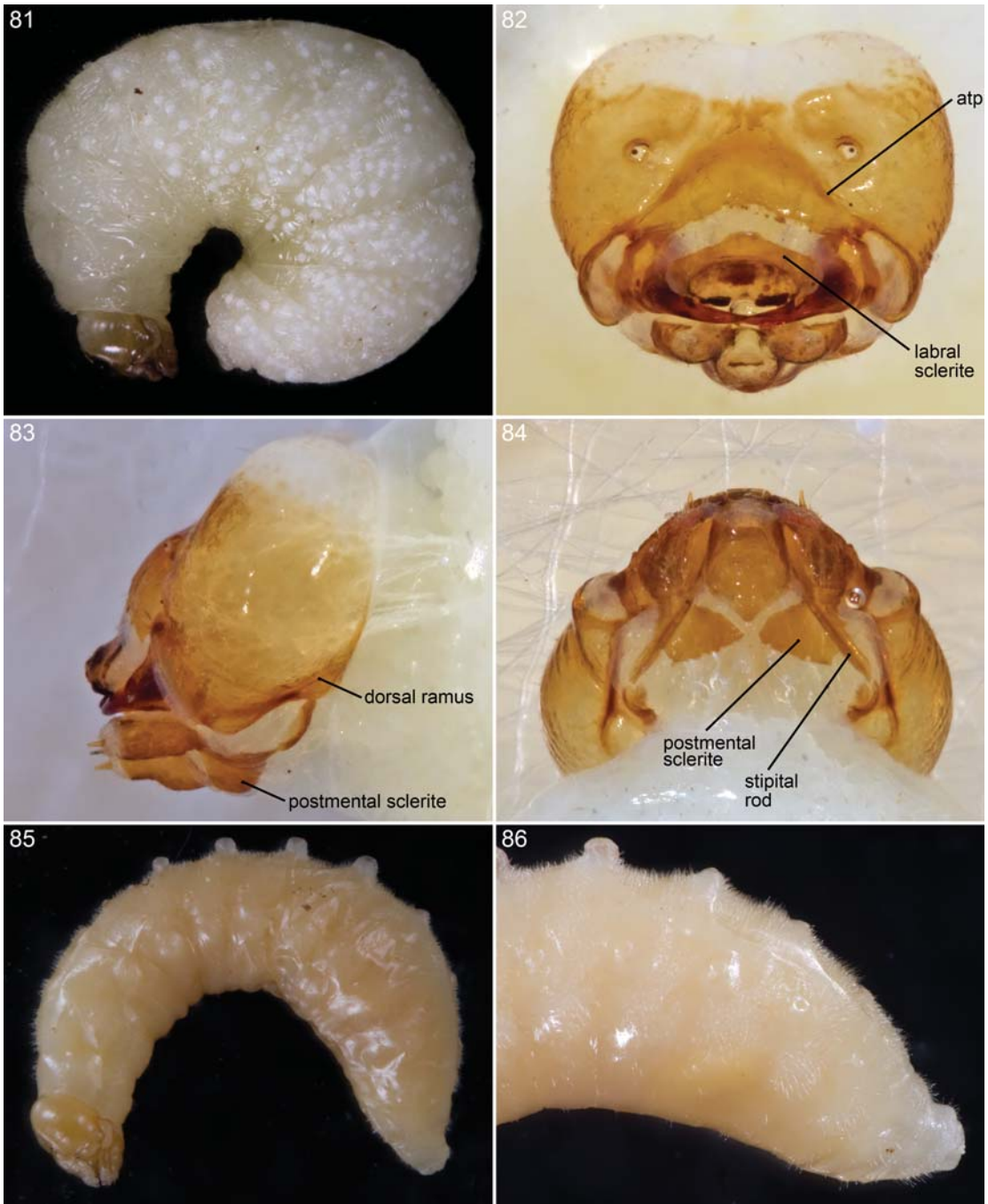
Figures 81–86, 94–97

The following is based on postdefecating and defecating (recently molted) forms.

DIAGNOSIS: The lack of a dorsal mandibular tooth will immediately distinguish the mature larva of *Stelis ater* from those of *S. elongativentris* (Rozen, 1987) and *S. murina* (Rozen and Kamel, 2009). The more extensive head pigmentation (figs. 82–84), the swollen pleurostomal area (figs. 82, 84, 95) as well as the pronounced basal ring to the antenna (figs. 95, 96) are additional helpful recognition features. The mature larva of *S. chlorocyanea* Cockerell (Rust and Thorp, 1973) and *S. lateralis* Cresson (Michener, 1953) also lacks a dorsal mandibular tooth but can apparently be distinguished from *S. ater* by their more elongate antennal papilla (Rust and Thorp, 1973: figs. 23, 25), which in *S. chlorocyanea* is twice as long as its basal diameter and in *S. lateralis* is closer to three times its basal diameter. The SEM figures of *S. chlorocyanea* indicate that it, like *S. ater*, has an elevated basal ring to the antenna and a somewhat swollen pleurostomal area. The specimen of *S. lateralis* described by Michener has a less conspicuous basal antennal ring and also a reduced pleurostomal swelling.

DESCRIPTION: Head (figs. 82–84): Setae moderately long, tapering to fine points; those of parietals scattered, suberect, with small alveoli; those of maxillary and labial apices straight, moderate in length, forward projecting and those of labral apex very small, downward directed. Following areas (figs. 82–84) tending to be heavily pigmented (compared to most bee larvae), with darker areas being dark brown (pigment fading with extensive boiling in aqueous solution of sodium hydroxide): lower half of parietals, entire frontal area, internal head ridges (especially pleurostomal, hypostomal, and lateral parts of epistomal ridges), clypeus, labrum, mandible, cardo, stipes, premental sclerite, large sclerotized area of each side of postmentum (figs. 83, 84); area on side of parietal above pigmented area with pigmented spots presumably associated with muscle attachment. Integumental spiculation absent except for fine spicules on hypopharyngeal lobes and perhaps maxillary apices.

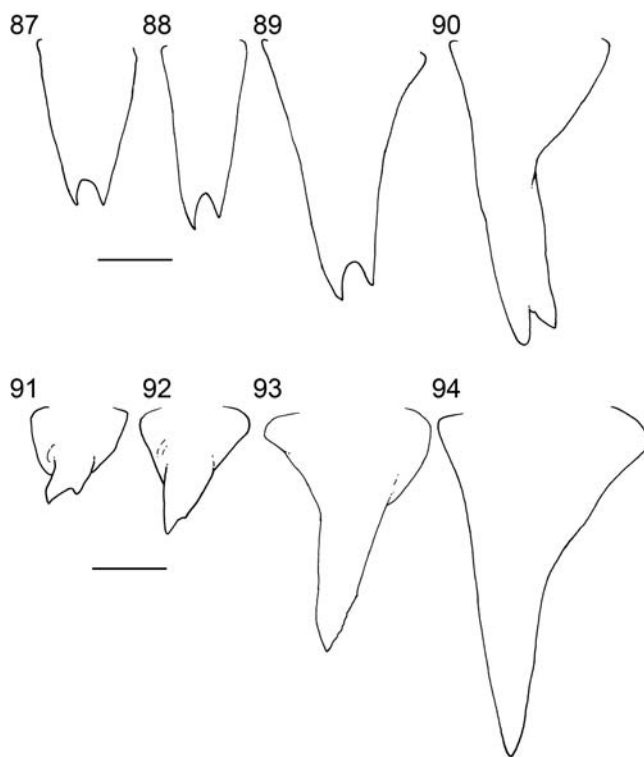
Parietals dorsolaterally swollen, so each side expands forward beyond midline, more so than in *Stelis murina* (Rozen and Kamel, 2009); maximum transverse diameter of head capsule to maximum transverse diameter of foramen 10:7; area immediately above hypostomal ridge and just behind posterior mandibular articulation not produced as downward-directed tubercle as present in many *Coelioxys* (Rozen and Kamel, 2007: fig. 47), but parietal approaching pleurostomal ridge somewhat flared (figs. 82, 84). Hypostomal ridge with dorsal ramus ending at postoccipital ridge (fig. 83); center of anterior tentorial pit closer to basal ring of antenna than to anterior mandibular articulation in anterior view; epistomal ridge absent mesad of anterior tentorial pits (atp, fig. 82); longitudinal thickening of head capsule (coronal ridge) present part-way to level of antennae. Parietal bands almost completely obscured by integumental scarring



FIGURES 81–86. Macroptic photographs of last larval instar of *Stelis ater*. **81.** Entire postdefecating form, lateral view. **82–84.** Head of same, front, dorsal, and ventral views, respectively; atp = anterior tentorial pit. **85.** Entire early fifth instar, lateral view. **86.** Posterior part of abdomen of another specimen, lateral view, showing segmentation of abdominal apex.

when viewed with stereomicroscope. Basal ring a strongly projecting ridge separated from the antennal papilla by unpigmented area (see Remarks, below); antennal papilla (fig. 96) small, apically narrowly rounded, about equal in length to basal diameter, bearing three, tightly grouped sensilla. Apical margin of clypeus evenly curved, so at midpoint its margin well below level of anterior tentorial pits as seen in frontal view. Labral sclerite pigmented, transverse (fig. 82) with pigmentation extending into apical sensilla-bearing area; apical labral margin concave, with lateral apical angles rounded; erect paired labral tubercles absent.

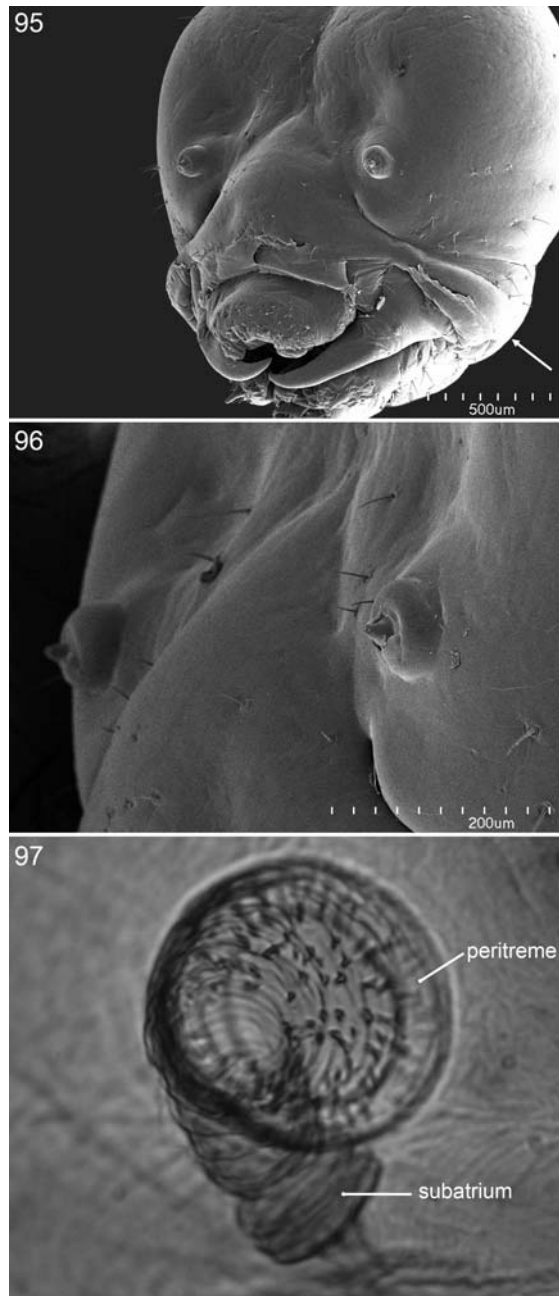
Mandible (fig. 94) elongate, apically robust but attenuate, strongly curved, tapering evenly to single apical point, almost certainly homolog of ventral tooth of *Stelis murina* (Rozen and Kamel, 2009: figs. 10, 11) and *S. elongativentris* (Rozen, 1987: fig. 11); inner surface without projecting cusp as seen in dorsal or ventral views but with apical concavity; concavity with irregular surface near base and bearing there several projections that are presumably not derived from dorsal apical tooth of other species since projection not on apical edge; outer mandibular surface with single seta not borne on tubercle. Cardo and stipes well developed, darkly pigmented; articulating arm of stipes arising from inner base of apical maxillary sclerite and extending just below hypopharyngeal lobe toward darkly pigmented premental bridge; maxillary palpus (fig. 84) slender, elongate, more than two times longer than basal diameter, much longer than antennal papilla. Apex of labium rather slender, with pronounced dorsally projecting, median swelling above salivary opening; labium clearly divided into prementum and postmentum; premental sclerite elongate, darkly pigmented on ventral surface, tapering from broad base to narrow apex; this sclerite apparently terminating apically, so it does not circle labial apex dorsally; at labial apex darkly pigmented premental bridge stretching across labial apex and nearly connecting with apices of premental sclerite; premental bridge with



FIGURES 87–90. Camera lucida illustrations of right larval mandible of *Osmia chalybea* stadia 2–5, respectively, outer view, with mandibular apex in approximate maximum profile; figures 87–89 are exoskeletons of a single individual, but figure 90 is from another individual. FIGURES 91–94. Camera lucida illustrations of right larval mandible of a single individual of *Stelis ater* stadia 2–5, respectively, outer view, with mandibular apex in approximate maximum profile; made from cast exoskeletons and preserved fifth instar. Scale bars = 0.1 mm.

pair of sublateral pigmented arms that extend forward before terminating (see Remarks, below); postmentum with pair of large, darkly pigmented sclerites that fuse laterally with stipital rods (see discussion of this feature in Rozen and Kamel, 2009: 15); labial palpi (fig. 84) subequal in length to maxillary palpi. Salivary lips projecting, broadly transverse, width about equal to distance between bases of labial palpi; inner surface of salivary lips not examined. Hypopharynx consisting of pair of well-separated, spiculate lateral lobes.

Body (figs. 81, 85, 86): Body setae abundant, moderately short; each seta without swollen base, tapering to fine apex; pleural area of abdominal segment 8 with approximately 40 setae; integument without spicules. Body of postdefecating forms (fig. 81) robust, flaccid, with abdominal segments 4–7 larger than other segments; intersegmental lines weakly incised mid-dorsally; intrasegmental lines of most segments quite evident on cleared specimen but difficult to identify on uncleared specimens; paired body tubercles absent; intersegmental body tubercles scarcely evident on postdefecating form (fig. 82); pleural swellings evident on most abdominal segments; abdominal segment 10 very short in lateral view, attached to approximate middle of segment 9, which is also short; anus transverse, projecting, positioned toward top of segment 10. Body of recently emerged fifth instar (figs. 85, 86) differing from that of postdefecating form as follows: slender, with abdominal segments 4–7 only slightly enlarged; intersegmental lines of anterior body segments moderately incised; those of most following segments poorly expressed dorsally since they pass through



FIGURES 95, 96. SEM micrographs of mature larva of *Stelis ater*. Head, anterolateral view, showing pronounced outer ring to antennae and swollen pleurostomal area (arrow), and close-up of antennae, respectively. FIGURE 97. Microphotograph of spiracle of cleared postdefecating larva of *Stelis ater* showing atrial wall, peritreme, and nearly parallel-sided subatrium.

exaggerated middorsal tubercles; intrasegmental lines moderately expressed at anterior end of body, becoming weaker posteriorly but evident owing to lack of expression of intersegmental lines there; body with middorsal, intersegmental tubercles as follows (fig. 85): between mesosoma and abdominal segment 1 (small), between abdominal segments 1 and 2, 2 and 3, 3 and 4, 4 and 5 (large), between 5 and 6, 6 and 7, 7 and 8 (becoming smaller); abdominal segment 10 longer ventrally than dorsally so that anus directed somewhat dorsally. Spiracles (fig. 97) well sclerotized, faintly pigmented, subequal in size; shallow, globular atrium projecting beyond body wall, with distinct rim (fig. 99); peritreme moderately narrow, so atrial opening about four times width of peritreme on one side; atrial inner surface with spines as long as width of peritreme, arranged in more or less concentric rows; these spines direct inward at right angles to atrial wall; primary tracheal opening perhaps with collar; subatrium moderately short, with perhaps 7–12 chambers; externally subatrial chambers of approximately uniform diameter from outer- to innermost chamber (i.e., sequence of chambers not tapering from outer- to innermost). Male of cleared specimen with median, transverse integumental scar close to posterior margin; female sex characters unknown.

MATERIAL STUDIED: Three newly emerged fifth instars and five postdefecating ones.

REMARKS: The basal ring of the antenna of *Stelis ater* (figs. 95, 96) projects strongly, even more so than that of *S. murina*, and much more so than that of *S. elongativentris*. This is an unusual feature; in most bee larvae the basal ring is merely the line where the sclerotization of the parietal stops and the membrane surrounding the base of the antennal papilla starts. In *S. ater* the sclerotization surrounding the membrane is extremely thick and outward projecting so the papilla and the basal membrane appear to be mounted on a tubercle (fig. 96).

The description of the labial apex differs substantially from that offered for *Stelis murina* (Rozen and Kamel, 2009) owing mainly to our examining a specimen cleared with lactic acid, which preserved the pigmentation. We strongly suspect that this feature in *S. murina* and *S. ater* are similar. However, the interpretation presented above is tentative. It is perhaps possible that the premental bridge identified above is in actuality merely the dorsal surface of the premental sclerite circling the labial apex despite apparent separation from the two dorsolateral edges of the premental sclerite.

The large projecting middorsal tubercles are an interesting feature. We wonder if they facilitate this instar's ability to crawl.

OTHER LARVAL INSTARS OF *OSMIA CHALYBEA* AND *STELIS ATER*

Early larval instars *Osmia chalybea* and *Stelis ater* are predictably similar to their last larval instars. The following account pertaining to mandibular features should aid in identifying their stage. Only the last (fifth) larval instar of each has conspicuous body setae and projecting salivary lips, hallmarks of last-stage larvae of higher megachilids.

In the case of *Osmia chalybea* the first larval instar has a linear band of spicules extending along each side of body just above the spiracular line (figs. 9, 10) and thus is unlike any of the following instars. As is also true for the cast first instar exoskeleton of *Stelis ater*, sclerotization

of the head capsule of *O. chalybea* is so weak that internal head ridges and mandibles cannot be identified on shed skins, probably a good indication that the larvae of both species remain pharate, wrapped immobile in the egg chorion, and the following instar is the first to actively feed on the provisions.

The mandible of the first larval instar of *Stelis ater* has not been identified but probably possesses two apical teeth, the presumed plesiomorphic condition for larval Megachilidae. The mandible of the second instar is clearly bidentate with both teeth acutely pointed and the ventral one longer (fig. 91). The mandible of the third instar (fig. 93) ends in a moderate-sized ventral tooth and small dorsal, almost obtusely angled tooth, the apical edge of which may have a slight serration. Fourth instar's mandible (fig. 94) ends in a single large, strong tooth irregularly serrated along the dorsal apical edge and perhaps with a slight dorsal swelling representing the dorsal apical tooth of early instars.

ACKNOWLEDGMENTS

Steve Thurston (Senior Scientific Assistant, AMNH) skillfully arranged and labeled all illustrative material for this report, expertly diagramed figures 17 and 43, and captured all Microptics images. SEM, X-ray, and CT-scan examination of specimens and cocoons was carried out in the AMNH Microscopy and Imaging Facility with the expert assistance of Rebecca Rudolph (Laboratory Manager) and Matthew Frenkel; Margaret A. Rozen, undergraduate volunteer, took all SEM micrographs and critical-pointed dried specimens beforehand.

Pavel B. Klimov identified mites found in nests of *Osmia chalybea*, and he and Barry M. O'Connor offered valuable insight into their biologies. John Sivinski provided tentative identification of *Melittobia digitata* Dahms, and Jorge González, kindly confirmed the determination. We thank Charles D. Michener for the long-term loan of the specimen of *Stelis lateralis* that he described more than a half a century ago.

Peter Frederick and Marilyn Spalding generously allowed access to their property along the southeast side of Kanapaha Prairie, where some of the trap nests were placed.

We thank John S. Ascher for the use of his photograph of adult *Stelis ater* (fig. 14) and Tim Lethbridge for the use of his picture of adult *Osmia chalybea* (fig. 11).

We extend our appreciation to John S. Ascher for his helpful review of the preliminary manuscript and also to Phillip Torchio both for reviewing the manuscript and for contributing his detailed, valuable insight gained through his years of studying the biology of *Osmia* and *Stelis*. Last but not least, thanks go to two anonymous reviewers for their keen eyes and valued suggestions.

REFERENCES

- Alexander, B., and J.G. Rozen, Jr. 1987. Ovaries, ovarioles, and oocytes in parasitic bees (Hymenoptera: Apoidea). *Pan-Pacific Entomologist* 63: 155–164.

- Alves dos Santos, I., G.A.R. Melo, and J.G. Rozen, Jr. 2002. Biology and immature stages of the bee tribe Tetrapedini (Hymenoptera: Apidae). *American Museum Novitates* 3377: 1–45.
- Baker, J.R. 1971. Development and sexual dimorphism of larvae of the bee genus *Coelioxys*. *Journal of the Kansas Entomological Society* 44: 225–235.
- Balfour[-]Browne, F. 1922. On the life history of *Melittobia acasta*, Walker: a chalcid parasite of bees and wasps. *Parasitology* 14: 23–371.
- Ferton, C. 1896. Nouvelles observations sur l'instinct des hyménoptères gastrilégides de la Provence. *Actes de la Société Linnéenne de Bordeaux* 48: 241–249, 1895.
- Hall, H.G., and J.S. Ascher. 2010. Surveys of bees (Hymenoptera: Apoidea: Anthophila) in natural areas of Alachua county in north-central Florida. *Florida Entomologist* 93: 609–629.
- Hawkins, W.A. 1975. Nesting biology of *Osmia (Chalcosmia) georgica* (Hymenoptera: Megachilidae). *Journal of the Kansas Entomological Society* 48: 493–499.
- Hurd, P.D. 1979. Superfamily Apoidea. In K.V. Krombein, P.D. Hurd, D.R. Smith, and P.D. Burks (editors), *Catalog of Hymenoptera in America north of Mexico*, Vol. 2: 1741–2209. Washington: Smithsonian Institution Press.
- Iwata, K., and S.F. Sakagami. 1966. Gigantism and dwarfism in bee eggs in relation to the modes of life, with notes on the number of ovarioles. *Japanese Journal of Ecology* 16: 4–16.
- Klimov, P.B., and B.M. O'Connor. 2008. Morphology, evolution, and host associations of bee-mites of the family Chaetodactylidae (Acari: Astigmata). *Miscellaneous Publications, Museum of Zoology, University of Michigan* 199: 1–243.
- Krombein, K. V. 1967. Trap-nesting wasps and bees: life histories, nests, and associates. Washington, DC: Smithsonian Press, i–vi, 1–570.
- Matthews, R.W., J.M. González, J.R. Matthews, and L.D. Deyrup. 2009. Biology of the parasitoid *Melittobia* (Hymenoptera: Eulophidae). *Annual Review of Entomology* 54: 252–266.
- Malyshev, S.I. 1935. The nesting habits of solitary bees. *EOS, Revista Española de Entomología* 11: 201–309, pls. 3–15.
- McGinley, R.J., and J.G. Rozen, Jr. 1987. Nesting biology, immature stages, and phylogenetic placement of the palaeartic bee genus *Pararhophites* (Hymenoptera: Apoidea). *American Museum Novitates* 2903: 1–21.
- Michener, C.D. 1953. Comparative morphology and systematic studies of bee larvae with a key to the families of hymenopterous larvae. *University of Kansas Science Bulletin* 35: 987–1102.
- Michener, C.D. 1955. Some biological observations on *Hoplitis pilosifrons* and *Stelis lateralis* (Hymenoptera, Megachilidae). *Journal of the Kansas Entomological Society* 28: 81–87.
- Michener, C.D. 2007. *The bees of the world*. 2nd ed. Baltimore, MD: Johns Hopkins University Press, 953 pp.
- Müller, A. 2010. Palaeartic osmiine bees. ETH Zürich. Internet resource (<http://blogs.ethz.ch/osmiini/>), accessed January, 2011.
- Parker, F.D. 1986. Nesting, associates, and mortality of *Osmia sanrafaelae* Parker. *Journal of the Kansas Entomological Society* 59: 367–377.
- Parker, F.D., J.H. Cane, G.W. Frankie, and S.B. Vinson. 1987. Host records and nest entry by *Dolichostelis*, a kleptoparasitic anthidiine bee (Hymenoptera: Megachilidae). *Pan-Pacific Entomologist* 63: 172–177.
- Rozen, J.G., Jr. 1970. Biology, immature stages, and phylogenetic relationships of fideliine bees, with the description of a new species of *Neofidelia* (Hymenoptera, Apoidea). *American Museum Novitates* 2427: 1–25.

- Rozen, J.G., Jr. 1987. Nesting biology of the bee *Ashmeadiella holtii* and its cleptoparasite, a new species of *Stelis* (Apoidea: Megachilidae). *American Museum Novitates* 2900: 1–10.
- Rozen, J.G., Jr. 2003. Eggs, ovariole numbers, and modes of parasitism of cleptoparasitic bees, with emphasis on Neotropical species (Hymenoptera: Apoidea). *American Museum Novitates* 3413: 1–36.
- Rozen, J.G., Jr., and S.L. Buchmann. 1990. Nesting biology and immature stages of the bees *Centris caesalpiniae*, *C. pallida*, and the cleptoparasite *Ericrocis lata* (Hymenoptera: Apoidea: Anthophoridae). *American Museum Novitates* 2985: 1–30.
- Rozen, J.G., Jr., and N.R. Jacobson. 1980. Biology and immature stages of *Macropis nuda*, including comparisons to related bees (Apoidea, Melittidae). *American Museum Novitates* 2702: 1–11.
- Rozen, J.G., Jr., and S.M. Kamel. 2007. Investigations on the biologies and immature stages of the cleptoparasitic bee genera *Radoszkowskiana* and *Coelioxys* and their *Megachile* hosts (Hymenoptera: Apoidea: Megachilidae: Megachilini). *American Museum Novitates* 3573: 1–43.
- Rozen, J.G., Jr., and S.M. Kamel. 2008. Hospicidal behavior of the cleptoparasitic bee *Coelioxys (Allocoelioxys) coturnix*, including descriptions of its early larval instars (Hymenoptera: Megachilidae). *American Museum Novitates* 3636: 1–15.
- Rozen, J.G., Jr., and S.M. Kamel. 2009. Last larval instar and mature oocyte of the Old World cleptoparasitic bee *Stelis murina*, including a review of *Stelis* biology. (Apoidea: Megachilidae: Megachilinae: Anthidiini). *American Museum Novitates* 3666: 1–24.
- Rozen, J.G., Jr., J.R. Rozen, and H.G. Hall. In prep. Gas diffusion rates through cocoon walls of two bee species (Hymenoptera: Megachilidae).
- Rozen, J.G., Jr., G.A.R. Melo, A.J.C. Aguiar, and I. Alves-dos-Santos. 2006. Nesting biologies and immature stages of the tapinotaspidine bee genera *Monoeca* and *Lanthanomelissa* and of their osirine cleptoparasites *Protosiris* and *Parepeolus* (Hymenoptera: Apidae). Appendix: Taxonomic notes on *Monoeca* and description of a new species of *Protosiris*, by G.A.R. Melo. *American Museum Novitates* 3501: 1–60.
- Rozen, J.G., Jr., S.B. Vinson, R. Coville, and G. Frankie. 2010a. Biology and immature stages of the cleptoparasitic bee *Coelioxys chichimeca* (Hymenoptera: Apoidea: Megachilidae). *American Museum Novitates* 3679: 1–26.
- Rozen, Jr., J.G., et al. 2010b. Nests, petal usage, floral preferences, and immatures of *Osmia (Ozbekosmia) avosetta* (Megachilidae: Megachilinae: Osmiini), including biological comparisons with other osmine bees. *American Museum Novitates* 3680: 1–22.
- Rust, R.W. 1974. The systematics and biology of the genus *Osmia*, subgenera *Osmia*, *Chalcosmia*, and *Cephalosmia* (Hymenoptera: Megachilidae). *Wasmann Journal of Biology* 32: 1–93.
- Rust, R.W., and R.W. Thorp. 1973. The biology of *Stelis chlorocyanea*, a parasite of *Osmia nigrifrons* (Hymenoptera: Megachilidae). *Journal of the Kansas Entomological Society* 26: 548–562.
- Sutherland, T.D., et al. 2007. Conservation of essential design features in coiled coil silks. *Molecular Biology and Evolution* 24: 2424–2432.
- Torchio, P.F. 1989a. In-nest biologies and development of immature stages of three *Osmia* species. (Hymenoptera: Megachilidae). *Annals of the Entomological Society of America* 82: 599–615.
- Torchio, P.F. 1989b. Biology, immatures, and adaptive behavior of *Stelis montana*, a cleptoparasite of *Osmia* (Hymenoptera: Megachilidae). *Annals of the Entomological Society of America* 82: 616–632.

Complete lists of all issues of *Novitates* and *Bulletin* are available on the web (<http://digitallibrary.amnh.org/dspace>). Inquire about ordering printed copies via e-mail from scipubs@amnh.org or via standard mail from:

American Museum of Natural History—Scientific Publications
Central Park West at 79th Street
New York, NY 10024

Ⓒ This paper meets the requirements of ANSI/NISO Z39.48-1992 (permanence of paper).